

CONTROL TECHNIQUES FOR DC-DC BUCK CONVERTER WITH IMPROVED PERFORMANCE

**A THESIS SUBMITTED IN PARTIAL FULFILLMENT
OF THE REQUIRMENTS FOR THE DEGREE OF**

Master of Technology (Research)

in

Electrical Engineering

by

Mousumi Biswal

(Roll: 608EE306)



**Department of Electrical Engineering
National Institute of Technology Rourkela**

March 2011

CONTROL TECHNIQUES FOR DC-DC BUCK CONVERTER WITH IMPROVED PERFORMANCE

A THESIS SUBMITTED IN PARTIAL FULFILLMENT
OF THE REQUIRMENTS FOR THE DEGREE OF

Master of Technology (Research)

in

Electrical Engineering

by

Mousumi Biswal

(Roll: 608EE306)



**Department of Electrical Engineering
National Institute of Technology Rourkela**

March 2011

CONTROL TECHNIQUES FOR DC-DC BUCK CONVERTER WITH IMPROVED PERFORMANCE

A THESIS SUBMITTED IN PARTIAL FULFILLMENT
OF THE REQUIRMENTS FOR THE DEGREE OF

Master of Technology (Research)

in

Electrical Engineering

by

Mousumi Biswal

Under the supervision of

Prof. Somnath Maity

and

Prof. Anup Kumar Panda



**Department of Electrical Engineering
National Institute of Technology Rourkela**

March 2011



DEPARTMENT OF ELECTRICAL ENGINEERING
NATIONAL INSTITUTE OF TECHNOLOGY, ROURKELA
ROURKELA-769008, ORISSA, INDIA

CERTIFICATE

This is to certify that the thesis entitled, “**Control Techniques for Dc/dc Buck Converter with Improved Performance**” submitted to the Department of Electrical Engineering, National Institute of Technology, Rourkela by Ms. Mousumi Biswal for the partial fulfillment of award of the degree Master of Technology (Research) is a bona fide record of research work carried out by her under our supervision and guidance.

The matter embodied in the thesis is original and has not been submitted elsewhere for the award of any degree or diploma.

In our opinion, the thesis is of standard required for the award of a Master of Technology (Research) Degree in Electrical Engineering.

Prof. Somnath Maity
(Supervisor)

Prof A. K. Panda
(Co-Supervisor)

ACKNOWLEDGEMENTS

I would like to express my heartiest gratitude towards my supervisor *Prof. (Dr.) Somnath Maity*, and my co-supervisor *Prof. (Dr.) A.K Panda*, Professor of Electrical Engineering for their valuable and enthusiastic guidance, help and continuous encouragement during the course of the present research work. I am indebted to them for having helped to shape the problem and providing insights towards the solution.

I am very much obliged to *Prof. (Dr.) B.D. Subudhi*, Professor and Head of the Department of Electrical Engineering for his valuable suggestions and support.

I am thankful to *Prof. (Dr.) K.B Mohanty*, Professor of Electrical Engineering and *Prof. (Dr.) Poonam Singh*, Professor of Electronics Engineering for their support during the research period.

I would like to give a special thanks to all my friends for all the thoughtful and mind stimulating discussions, sharing of knowledge which prompted us to think beyond. The help and co-operation received from the staff of Department of Electrical Engineering is thankfully acknowledged.

I would like to thank my parents for their prayer, understanding and moral support during the tenure of research work.

Mousumi Biswal

ABSTRACT

The switched-mode dc-dc converters are some of the most widely used power electronics circuits for its high conversion efficiency and flexible output voltage. These converters used for electronic devices are designed to regulate the output voltage against the changes of the input voltage and load current. This leads to the requirement of more advanced control methods to meet the real demand. Many control methods are developed for the control of dc-dc converters. To obtain a control method that has the best performances under any conditions is always in demand.

Conventionally, the dc-dc converters have been controlled by linear voltage mode and current mode control methods. These controllers offer advantages such as fixed switching frequencies and zero steady-state error and gives a better small-signal performance at the designed operating point. But under large parameter and load variation, their performance degrades. Sliding mode (SM) control techniques are well suited to dc-dc converters as they are inherently variable structure systems. These controllers are robust concerning converter parameter variations, load and line disturbances. SM controlled converters generally suffer from switching frequency variation when the input voltage and output load are varied. This complicates the design of the input and output filters. The main objective of this research work is to study different control methods implemented in dc-dc converter namely (linear controllers, hysteresis control, current programmed control, and sliding mode (SM) control). A comparison of the effects of the PWM controllers and the SM control on the dc-dc buck converter response in steady state, under line variations, load variations is performed.

The thesis shows that, in comparison with the PWM controllers, the SM control provides better steady-state response, better dynamic response, and robustness against system uncertainty disturbances. Also the hysteretic controlled converters response to disturbances and load change right after the transient take place and they give excellent transient performance. It does not require the closed loop compensation network and results with a lesser component count and small size in implementation. Hence, hysteretic control is considered as the simplest and fastest control method. The dc-dc buck converter employing current hysteresis control scheme is given in thesis. The result shows that hysteresis control converters have inherently fast response and they are robust with simple design and implementation.

A hysteretic current control technique for a tri-state buck converter operating in constant switching frequency is designed and its behavior is studied by making the use of essential tools of sliding mode control theory because dc-dc buck converter is a variable structure system due to the presence of switching actions. The principle of operation of tristate dc-dc buck converter is explained. The converter response is investigated in the steady-state region and in the dynamic region. The problem of variable switching frequency is eliminated without using any compensating ramp.

Keywords: Hysteresis control, Sliding mode control, Dc-dc buck converter, variable structure system.

CONTENTS

Title	Page No.
Certificate	i
Acknowledgement	ii
Abstract	iii
Contents	v
List of Figures	viii
Nomenclature	x
Abbreviations	xii

CHAPTER 1: INTRODUCTION

1.1	Motivation	1
1.2	Literature Review	4
1.3	Basic Principles of Sliding-mode Control	10
1.4	Review on Sliding-mode Control Theory	11
1.5	Objective and Scope of this Dissertation	15
1.6	Organization of Thesis	16

CHAPTER 2: CONTROL METHODS FOR DC-DC CONVERTER

2.1	Introduction	17
2.2	The Dc-dc Buck Converter	18
2.3	Modes of Operation of Dc-dc Buck Converter	20
	2.3.1 Continuous Conduction Mode (CCM)	20
	2.3.2 Discontinuous Conduction Mode (DCM)	21

2.4	Control Methods for Dc-dc Converter	22
2.4.1	Voltage-Mode Controlled Buck Converter	22
2.4.2	Current-Mode Controlled Buck Converter	25
2.5	Sliding-mode control for Dc-dc Buck Converter	29
2.5.1	System Modeling	29
2.5.2	Design of SM Controller	31
2.5.3	Derivation of SM Existence Condition	33
2.6	Simulation Results	38
2.7	Conclusion	45

CHAPTER 3: FIXED FREQUENCY HYSTERESIS CONTROLLER

3.1	Introduction	46
3.2	Variable switching Frequency Hysteretic Controllers	47
3.2.1	Hysteretic Voltage-Mode Controllers	47
3.2.2	Hysteretic Current-Mode controllers	48
3.3	Simulation Results	50
3.4	Constant Switching Frequency Current-mode Hysteretic Controller	54
3.4.1	Basic Concept of Operation	54
3.4.2	Mathematical Analysis of proposed Controller	57
3.5	Model including parasitic elements	64
3.6	Simulation Results	65
3.7	Conclusion	74

CHAPTER 4: CONCLUSIONS AND FUTURE SCOPES

4.1	Conclusions	71
4.2	Scope for Future work	73
	REFERENCES	74

LIST OF FIGURES

Figure	Title	Page
Figure 1.1(a)	Phase Plot for ideal SM Control	10
Figure 1.1(b)	Phase Plot for actual SM control	10
Figure 2.1	Buck dc-dc converter topology	18
Figure 2.2(a)	Buck Converter when switch turns on	19
Figure 2.2(b)	Buck Converter when switch turns off	19
Figure 2.3(a)	Inductor current waveform of PWM converter in CCM	21
Figure 2.3(b)	Inductor current waveform of PWM converter in the boundary of CCM and DCM	21
Figure 2.3(c)	Inductor current waveform of PWM converter in DCM	21
Figure 2.4	Block diagram of voltage mode controller	22
Figure 2.5	Current-mode controlled dc-dc buck converter	25
Figure 2.6	Peak Current Mode Control	28
Figure 2.7	Inductor Current waveform with compensating ramp	28
Figure 2.8	Basic structure of an SMC buck converter system	29
Figure 2.9	Sliding line on $x_1 - x_2$ phase plane	33
Figure 2.10	Region of Existence of SM mapped in the phase plane	35
Figure 2.11	Evolution of phase trajectory in phase plane for $c_1 > c_2/RC$	35

Figure 2.12	Phase plane diagram for $c_1 > c_2/RC$	36
Figure 2.13	Phase plane diagram for $c_1 < c_2/RC$	36
Figure 2.14	Chattering phenomena of SM control	37
Figure 2.15	Output Voltage response due to a step change in load resistance from 15Ω to 10Ω and back to 15Ω	39
Figure 2.16	Inductor Current response due to a step change in load resistance from 15Ω to 10Ω and back to 15Ω	39
Figure 2.17	Output Voltage response for a change input voltage from 20V to 15V and back to 20V	40
Figure 2.18	Inductor Current response for a change input voltage from 20V to 15V and back to 20V	40
Figure 2.19	Output Voltage response due to a step change in load resistance from 15Ω to 10Ω and back to 15Ω	42
Figure 2.20	Inductor Current response due to a step change in load resistance from 15Ω to 10Ω and back to 15Ω	42
Figure 2.21	Output Voltage response for a change input voltage from 20V to 15V and back to 20V	43
Figure 2.22	Inductor Current response for a change input voltage from 20V to 15V and back to 20V	43
Figure 2.23	Phase plane plot under step load transient from for SM control	44
Figure 3.1	Voltage hysteresis control	47
Figure 3.2	Hysteretic CM controlled buck converter	48

Figure 3.3	Transient response of the hysteretic current controlled buck converter when load from 15Ω to 10Ω and back to 15Ω	51
Figure 3.4	Transient response of the hysteretic current controlled buck converter when input voltage from 20V to 15V and back to 20V	52
Figure 3.5	Phase plane diagram with load transient	53
Figure 3.6	A tristate buck converter configuration	55
Figure 3.7(a)	Equivalent circuits under different modes of operation: mode 1 (D_1T_s)	55
Figure 3.7(b)	Equivalent circuits under different modes of operation: mode 2 (D_2T_s)	55
Figure 3.7(c)	Equivalent circuits under different modes of operation: mode 3 (D_3T_s)	56
Figure 3.8	Inductor current waveform of a tristate buck converter showing the switch conditions	57
Figure 3.9	Schematic diagram of the hysteretic controller for tristate buck converter	57
Figure 3.10	Schematic diagram of pulse generator circuit	58
Figure 3.11	Model of tristate buck converter with all parasitic elements	64
Figure 3.12	Startup transient performance of converter with the proposed controller	66
Figure 3.13	The proposed current hysteretic controller operating principle	67
Figure 3.14	Transient response for a change in load from 15Ω to 10Ω and back to 15Ω	68

Figure 3.15	Output voltage response from load transient 10Ω to 15Ω	68
Figure 3.16	Load transient response from 15Ω to 10Ω	69
Figure 3.17	Load transient response from 15Ω to 10Ω for conventional current hysteretic control method	69
Figure 3.18	Transient response due to a step change in reference voltage from $6V$ to $5V$ and back to $6V$	70
Figure 3.19	Phase plane diagram	71
Figure 3.20	Magnified view showing the phase trajectory and hysteresis band	71
Figure 3.21	The output voltage ripple and inductor current ripple in steady state operation by considering the effect of parasitic elements	72
Figure 3.22	The inductor current ripple in steady state operation	73

NOTATIONS

Symbol

x	State vector
f	Function vector with n-dimension
u	Discontinuous control input
S	Sliding surface (manifold)
f^+, f^-	State velocity vector
f_N^+, f_N^-	Normal vectors
∇S	Gradient of sliding surface
e^+, e^-	Representative points
φ	Constant value
u_{eq}	Equivalent continuous control input
S_w	controlled switch
L	Inductance
C	capacitance
R	Load resistance
i_L	Inductor current
i_C	Capacitor current
v_C	Capacitor voltage

v_{in}	Input voltage
v_0	Output voltage
v_{con}	Control voltage
V_{ref}	Reference voltage
k_p, k_I	Proportional gain and integral gain of P-I controller
k_1	Voltage reduction factor
v_{ramp}	Sawtooth or Ramp voltage
V_U, V_L	Upper and Lower threshold voltages
q	Switching signal
h	Switching hypersurface
i_{ref}	Reference current
R_f	Proportionality factor
x_1	Voltage error
x_2	Voltage error dynamics
λ_1, λ_2	Line equations in phase plane
Δ	Small constant value
D	Diode
f_s	Switching frequency
T_s	Time period of external clock pulse

ABBREVIATIONS

SMPS	Switched Mode Power Supply
CCM	Continuous Conduction Mode
DCM	Discontinuous Conduction Mode
SM	Sliding Mode
VSC	Variable Structure Control
VSS	Variable Structure System
P	Proportional Control
PD	Proportional derivative Control
PID	Proportional integral derivative Control
EMI	Electromagnetic Interference
HM	Hysteresis Modulation
PWM	Pulse Width Modulation
GPI	Generalized proportional integral
PCCM	Pseudo continuous conduction mode
RP	Representative Point
VMC	Voltage mode control
CMC	Current mode control
PCMC	Peak current mode control

Chapter 1

CHAPTER 1

Introduction

1.1 Motivation

The switched mode dc-dc converters are some of the simplest power electronic circuits which convert one level of electrical voltage into another level by switching action. These converters have received an increasing deal of interest in many areas. This is due to their wide applications like power supplies for personal computers, office equipments, appliance control, telecommunication equipments, DC motor drives, automotive, aircraft, etc. The analysis, control and stabilization of switching converters are the main factors that need to be considered. Many control methods are used for control of switch mode dc-dc converters and the simple and low cost controller structure is always in demand for most industrial and high performance applications. Every control method has some advantages and drawbacks due to which that particular control method consider as a suitable control method under specific conditions, compared to other control methods. The control method that gives the best performances under any conditions is always in demand.

The commonly used control methods for dc-dc converters are pulse width modulated (PWM) voltage mode control, PWM current mode control with proportional (P), proportional integral (PI), and proportional integral derivative (PID) controller. These conventional control methods like P, PI, and PID are unable to perform satisfactorily under large parameter or load variation. Therefore, nonlinear controllers come into

picture for controlling dc-dc converters. The advantages of these nonlinear controllers are their ability to react suddenly to a transient condition. The different types of nonlinear controllers are hysteresis controller, sliding mode controller, boundary controller, etc.

The hysteresis control methods for power converters are also gaining a lot of interest due its fast response and robust with simple design and implementation. The hysteresis controllers react immediately after the load transient takes place. Hence the advantages of hysteretic control over other control technique include simplicity, do not require feedback loop compensation, fast response to load transient. However, the main factors need to be considered in case of hysteresis control are variable switching frequency operation and stability analysis.

The dc-dc converters, which are non-linear and time variant system, and do not lend themselves to the application of linear control theory, can be controlled by means of sliding-mode (SM) control, Which is derived from the variable structure control system theory (VSCS). Variable structure systems are systems the physical structures of which are changed during time with respect to the structure control law. The instances at which the changing of the structure occurs are determined by the current state of the system. Due to the presence of switching action, switched-mode power supplies (SMPS) are generally variable structured systems. Therefore, SM controllers are used for controlling dc-dc converters.

SM control method has several advantages over the other control methods that are stability for large line and load variations, robustness, good dynamic response, simple implementation. Ideally, SM controllers operate at infinite switching frequency and the controlled variables generally track a particular reference path to achieve the desired steady state operation. But an infinite switching frequency is not acceptable in practice, especially in power electronic circuits and therefore a control technique that can ensure a

finite switching frequency must be implemented. The extreme high speed switching operation results in switching losses, inductor and transformer core loss and electromagnetic-interference (EMI) generation. Variable switching frequency also complicates the design of input and output filter. Hence, for SM controllers to be applicable to dc-dc converters, their switching frequency should be constricted within a practical range.

Though SM control compiles of various advantages, SM controlled converters suffers from switching frequency variation when the input voltage and output load are varied. Hence there are many control methods which have been developed for fixed switching frequency SM control such as fixed frequency PWM based sliding mode controllers, adaptive SM controller, digital fuzzy logic SM controller, etc. In case of adaptive control, adaptive hysteresis band is varied with parameter changes to control and fixate the switching frequency. But, these methods require more components and are unattractive for low cost voltage conversion applications.

The different types of hysteresis controller are hysteretic voltage-mode controller, V^2 controller, and hysteretic current-mode controllers. The current hysteresis control incorporates both the advantages of hysteresis control and current mode control. It can be implemented using two loop control method. The error between the actual output voltage and reference voltage gives the error voltage. A PI control block can use the voltage error signal to provide a reference current for hysteresis control. This is also called sliding mode control for dc-dc converter. Therefore, the current mode hysteretic controller can be considered as a sliding mode control system and the analysis of hysteretic controller can be done as per sliding mode control theory. The essential tools of this nonlinear control theory can be introduced for the study of the behavior of hysteresis controller.

Therefore, the motivation of this thesis is to improve the performance of a dc-dc buck converter through controller improvements. Hence, this thesis focused on the design and analysis of a fixed frequency hysteretic current mode controller with improved performance for dc-dc buck converter circuit. The problem of switching frequency variation is alleviated with simplicity in controller design.

1.2 Literature Review

The dc-dc switching converters are the widely used circuits in electronics systems. They are usually used to obtain a stabilized output voltage from a given input DC voltage which is lower (buck) from that input voltage, or higher (boost) or generic (buck–boost) [1]. Most used technique to control switching power supplies is Pulse-width Modulation (PWM) [2]. The conventional PWM controlled power electronics circuits are modeled based on averaging technique and the system being controlled operates optimally only for a specific condition [3]-[4]. The linear controllers like P, PI, and PID do not offer a good large-signal transient (i.e. large-signal operating conditions) [4]-[5].

Therefore, research has been performed for investigating non-linear controllers. The main advantages of these controllers are their ability to react immediately to a transient condition. The different types of non-linear analog controllers are: (a) hysteretic current-mode controllers, (b) hysteretic voltage-mode/V2 controllers, (c) sliding-mode/boundary controllers. Advantages of hysteretic control approach include simplicity in design and do not require feedback loop compensation circuit. M. Castilla [6]-[8] proposed voltage-mode hysteretic controllers for synchronous buck converter used for many applications. The analysis and design of a hysteretic PWM controller with improved transient response have been proposed for buck converter in 2004[9].

The use of SM control techniques in variable structure systems (VSS) makes these systems robust to parameter variations and external disturbances [10]-[11]. Sliding mode control has a high degree of design flexibility and it is comparatively easy to implement. This explains its wide utilization in various industrial applications, e.g. automotive control, furnace control, etc. [10]-[12]. Switched mode dc-dc converters represent a particular class of the VSS, since their structure is periodically changed by the action of controlled switches and diodes. So it is appropriate to use sliding mode controllers in dc-dc converters [13]. It is known that the use of SM (nonlinear) controllers can maintain a good regulation for a wide operating range. So, a lot of interest is developed in the use of SM controllers for dc-dc converters [14]-[63]. Siew-Chong Tan presented a detail discussion on the use of SM control for dc-dc power converters [15].

In 1983 and 1985, the implementation of sliding mode control for dc-dc converters is first presented [13]-[14]. Then SM controller is applied in higher order converters in 1989 [16]. Huang *et al.* applied SM control for cuk switching regulator. After this, a series of related works on the cuk converter was carried out [17]-[20]. Fossas and Pas [21] applied a second-order SM control algorithms to buck converter for reduction of chattering. Then, two types of SM-control for boost and buck-boost converters: one using the method of stable system centre [22] and the other using sliding dynamic manifold [23] is proposed by Yuri B. Shtessel. Sira-Ramirez [24] proposed a hysteresis modulation type of SM controller to achieve a generalized proportional integral (GPI) continuous control of a buck converter. Sira-Ramirez also presented a tutorial revisit of traditional sliding mode control approach for the regulation of dc-dc power converters, of the ‘buck’, ‘boost’ and ‘buck-boost’ type and proposed the use of GPI control technique to improve system robustness [25].

Raviraj and Sen presented a comparative study on buck converter's performance when controlled by PI, SM, and fuzzy-logic controllers in 1997 [26]. They showed that there are certain similarities in the system behavior between fuzzy-logic and SM controllers. SM controller is also applied on parallel connected dc-dc converters. Donoso-Garcia *et al.* [27] and Shtessel *et al.* [28] proposed the use of SM control for current distribution and output-voltage regulation of multiple modular dc-dc converters. Sira-Ramirez and Rios-Bolivar [29] applied extended linearization method in SM-controller design that has excellent self scheduling properties. They also proposed to combine a SM control scheme with passivity-based controllers into the dc-dc converter that enhances its robustness properties [30]-[31]. In 1997, Carrasco *et al.* [32] proposed neural controller with SM controllers to improve the robustness, stability and dynamic characteristic of the PWM dc/dc power circuit with power factor corrector.

The nonlinear behavior exhibited by current mode controlled boost converter is studied by Morel [33]-[35]. Then, he introduced a practical SM control method aiming to eliminate chaotic behavior and keep the desired current-controlled property. The standard method (slope compensation) only partly cures this major drawback and, even though it eliminates chaos, the converter is not current-controlled any more. He concluded that the proposed method does not only provide stability, it also increases the input voltage variation domain for which the system remained stable.

Mattavelli *et al.* [36] proposed a general-purpose sliding-mode controller, which is applicable to most dc-dc converter topologies. The circuit complexity is same as current-mode controllers and it provides extreme robustness and speed of response against line, load and parameter variations. The same group derived small signal models for dc-dc converters with SM control, which allows the selection of control coefficients, the analysis of parameter variation effects, the evaluation of the closed loop performances

like audio susceptibility, output and input impedances, and reference to output transfer function [37].

Despite various advantages of SM controller, the practical implementation of this controller for dc-dc converters is rarely discussed. This is due to the lack of understanding in its design and systematic procedure for developing such controllers. Escobar *et al.* [38] performed experiments to compare five different control algorithms on dc-dc boost converter. He concluded that nonlinear controllers provide a promising alternative to the linear average controller. Alarcon *et al.* [39] presented the design of analog IC SM control prototype with linear sliding surface for switching converters. Ahmed *et al.* [40], [41] presented an analysis and experimental study of SM controlled buck converter. They also showed the implementation of the SM controller for buck-boost converter through control desk dSPACE [42]. Dominguez *et al.* [43] presented a stability analysis of buck converter with input filter by means of SM control technique. Zhang li and QIU Shui-sheng implemented Proportional-Integral sliding mode controller in dc-dc converters. They showed that the implementation of PI SM control is simpler than other SM control schemes and steady state error is eliminated [44]. Castilla *et al.* [45] created a novel design methodology of SM control schemes for quantum resonant converters. The method is based on the imposition of a specified output-voltage dynamic response, and it provides a set of sliding surfaces guaranteeing high robustness and large signal stability. Siew-Chong Tan presented a systematic approach for designing a practical SM controller for buck converter [46].

An ideal SMCT (sliding mode control technique) operates at infinite switching frequency [46]-[47]. This infinite switching frequency invites inductor, transformer core losses and electromagnetic interference noise issues. Hence, practical SM controllers are operated at finite switching frequencies only. Thus, ideal SM is brought to quasi-sliding

mode. The frequency limited SM controllers are generally called as Quasi-sliding mode controllers [47]. Cardoso *et al.* [48] proposed several methods to constrict the switching frequency of the SM controlled converters. Switching frequency variation can be eliminated by employing PWM based SM control instead of hysteresis modulation (HM) [49].

Nguyen and Lee proposed an adaptive hysteresis type of SM controller for buck converter [50]. They again proposed an indirect implementation of SM controllers in buck converter to achieve constant switching frequency operation [51]. Chiacchiarini *et al.* [52] performed experiment to compare the performance of buck converter controlled by analog and also for digital sliding-mode controllers. Sira-Ramirez *et al.* [53] proposed a geometric approach to map the PWM feedback control onto SM control and provide the equivalence between SM and PWM controller [54]. The discrete control input is replaced by a smooth analytic function of the state, known as the duty ratio.

Mahadevi *et al.* [55] proposed state space averaging method to PWM based SM controlled dc-dc converters with a constant switching frequency. They also applied neural networks into their PWM-based SM controlled converters [56]. Siew-Chong Tan proposed a new adaptive sliding mode controller for buck converter in continuous conduction mode of operation [57]. They concluded that adaptive SM controlled converter has faster dynamic response with reduced steady state error when it operated above the nominal load, and it eliminates overshoots and ringing in the transient response when operated below the nominal load. In 2004, a digital fuzzy logic SM-like controller that has zero steady state error and fixed switching frequency is proposed by Perry *et al.* [58]. Ianneli and Vasca proposed method of dithering to SM controlled converters for maintaining a finite and constant switching frequency [59].

Steady-state switching frequency of sliding mode controlled dc-dc converters is generally affected by line and load variation. For line variation, an adaptive feed forward control that varies the hysteresis band in the hysteresis modulator of the SM controller in the event of any change of the line input voltage and for load variation, an adaptive feedback controller that varies the control parameter with the change of output load is proposed by Siew-Chong Tan [60]. Dc-dc converters can be operated either in continuous conduction mode (CCM) or in discontinuous conduction mode (DCM). Dc-dc converters that operated in DCM provide faster transient response (due to its low inductance) at the expense of higher device stresses. He also presented a fixed frequency PWM based sliding mode controllers for dc-dc converters operating in DCM [62]-[63].

Buck converter when operated in CCM, gives a continuous output current, with smaller current ripple and low switching noise. CCM operation is usually preferred for large current applications, because it can deliver more current than the converter operating in DCM. However, a DCM converter has a much faster transient response and a loop gain that is easier to compensate than a CCM converter. Hence, for fulfill of both the requirements, a new converter that combines the advantage of both CCM and DCM converters is developed. Converters operate in a new operation mode-the pseudo CCM. This new switching converter that is operating in pseudo-continuous-conduction-mode (PCCM) with freewheel switching control is proposed by Dongsheng Ma and Wing-Hung Ki [64]-[65]. They showed that pseudo CCM buck converter has much improved current handling capability with reduced current and voltage ripple.

1.3 Basic principles of SM control

The basic idea of SM control is to design first a sliding surface in state space and then the second is to design a control law direct the system state trajectory starting from any arbitrary initial state to reach the sliding surface in finite time, and finally it should come to a point where the system equilibrium state exists that is in the origin point of the phase plane. The existence, stability and hitting condition are the three factors for the stability of sliding mode control. SM control principle is graphically represented in Figure 1, where $S=0$, represent the sliding surface and x_1 and x_2 are the voltage error variable and voltage error dynamics respectively. The sliding line (when it is a two variable SM control system in two-dimensional plane) divides the phase plane into two regions. Each region is specified with a switching state and when the trajectory arrives at the system equilibrium point, the system is considered as stable.

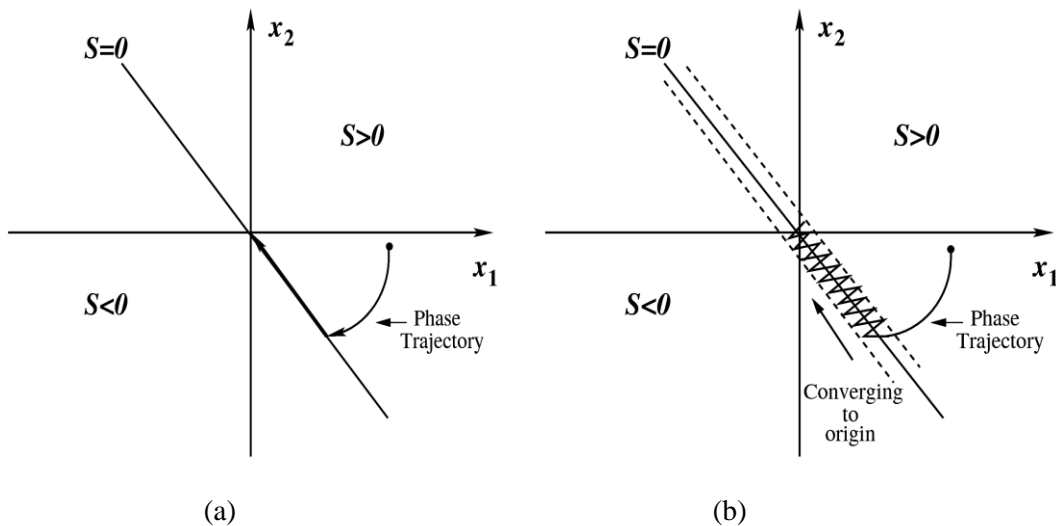


Figure 1.1: Phase Plot for (a) ideal SM Control (b) actual SM control

If the hysteresis band around the sliding line becomes zero, then system is said to be operated with ideal SM control. But, from the practical point of view, this is not possible

to achieve. Hence, the actual SM control operation that is when the hysteresis band is not ideal having a finite switching frequency is shown in figure 1.1(b) [46].

1.4 Review on SM control theory

The SM control theory is a well discussed topic [12], [61]. In this section a general review on SM control theory is presented. Let us consider a general system with scalar control as an example for better understanding of design procedure of SM control.

$$\frac{dx}{dt} = f(x, t, u) \quad (1.1)$$

where x is the column vector that represents the state of the system, f is a function vector with n dimension, u is the control input that makes the system discontinuous. The function vector f is discontinuous on the sliding surface $S(x, t) = 0$, which can be represented as,

$$f(x, t, u) = \begin{cases} f^+(x, t, u^+) & \text{for } S(x, t) > 0 \\ f^-(x, t, u^-) & \text{for } S(x, t) < 0 \end{cases} \quad (1.2)$$

where $S(x, t) = 0$ is the sliding surface (sliding manifold). The system is in sliding mode if its representative point (RP) moves on the sliding surface $S(x, t) = 0$.

Existence condition and reaching condition are two requirements for a stable SM control system. The existence condition of sliding mode requires that the phase trajectories belongs to the two regions, created by the sliding line, corresponding to the two different values of the vector function f must be directed towards the sliding line. While approaching the sliding line from the point which satisfies $S(x, t) > 0$, the corresponding state velocity vector f^+ must be directed toward the sliding surface, and

the same happens for the points above $S(x,t) < 0$ for which the corresponding state velocity vector is f^- .

The normal vectors (f_N^+, f_N^-) of the function f are orthogonal to the sliding surface or the sliding line, which is given by,

$$\begin{aligned} \lim_{S \rightarrow 0^+} f_N^+ < 0 &\Rightarrow \lim_{S \rightarrow 0^+} \nabla S \cdot f^+ < 0 \\ \lim_{S \rightarrow 0^-} f_N^- > 0 &\Rightarrow \lim_{S \rightarrow 0^-} \nabla S \cdot f^- > 0 \end{aligned} \quad (1.3)$$

where ∇S is the gradient of surface S . This is expressed as

$$\frac{dS}{dt} = \sum_{i=1}^N \frac{\delta S}{\delta x_i} \frac{dx_i}{dt} = \nabla S \cdot f \quad (1.4)$$

Therefore, in mathematical terms the sliding-mode existence condition is represented as

$$\lim_{S \rightarrow 0} S \frac{dS}{dt} < 0 \quad (1.5)$$

When the inequality given in equation (2.5) holds in the entire state space, then this is the sufficient condition for the system RP to reach the sliding surface.

The reaching condition means the system RP will reach the sliding surface within finite time interval. The scalar discontinuous input u at any instant depends upon the system RP in state space at that instant. Hence, the control input for the system in (1.1) can be written in mathematical form as,

$$u = \begin{cases} u^+ & \text{for } S(x,t) > 0 \\ u^- & \text{for } S(x,t) < 0 \end{cases} \quad (1.6)$$

where u^+ and u^- are the switching states which belong to the region $S(x) > 0$ and $S(x) < 0$ respectively. Let $[e^+]$ and $[e^-]$ be the steady state RPs corresponding to the

inputs u^+ and u^- . Then a sufficient condition for reaching the sliding surface is given by:

$$\begin{aligned} [e^+] \in S(x,t) < 0 \\ [e^-] \in S(x,t) > 0 \end{aligned} \quad (1.7)$$

If the steady state point for one substructure belongs to the region of phase space reserved to the other substructure, then sooner or later the system RP will hit the sliding surface.

Then, the behavior of dc-dc switching converter when operated in sliding mode with the equivalent input is described below.

For the dc-dc converter system the state space model can be written as,

$$\frac{dx}{dt} = f(x,t) + g(x,t)u \quad (1.8)$$

The control input u is discontinuous on sliding surface $S(x,t) = 0$, while f and g are continuous function vectors. The sliding surface is a combination of state variables as

$$S(x,t) = kx + \varphi \quad (1.9)$$

Under SM control, the system trajectories stay on the sliding surface, therefore:

$$\begin{aligned} S(x,t) &= 0 \\ \Rightarrow \frac{d}{dt} S(x,t) &= 0 \end{aligned} \quad (1.10)$$

$$\begin{aligned} \frac{dS}{dt} &= \sum_{i=1}^n \frac{\partial S}{\partial x_i} \frac{dx_i}{dt} \\ &= \nabla S \frac{dx}{dt} \\ &= k \frac{dx}{dt} \end{aligned} \quad (1.11)$$

where k is a 1 by n matrix, the elements of which are the derivatives of the sliding surface with respect to the state variables (gradient vector) and φ is some constant value.

Using equations (1.8) and (1.11) leads to

$$k \frac{dx}{dt} = kf(x,t) + kg(x,t)u_{eq} = 0 \quad (1.12)$$

where the discrete control input u was replaced by an equivalent continuous control input u_{eq} , which maintains the system evolution on the sliding surface. The expression for the equivalent control is given as

$$u_{eq} = -(kg)^{-1}kf(x,t) \quad (1.13)$$

Substituting equation (1.13) into equation (1.8) gives

$$\frac{dx}{dt} = [I - g(kg)^{-1}k]f(x,t) \quad (1.14)$$

Equation (1.14) describes the system motion under the SM control. The system should be stable around any operating point. For satisfying the stability condition of the SM control, the created sliding surface will always direct the state trajectory towards a point where system stable equilibrium exists. This is generally accomplished through the design of the sliding coefficients to meet the desired dynamical property. This is possible by using the invariance property. Since in sliding mode operation, the state trajectory will track the path of the sliding surface to a point of stability, the dynamical property of the system can be determined by proper selection of sliding coefficient.

1.5 Objective and Scope of this Dissertation

Control of switching converters is an interesting research area. The dynamic performance improvement and stability of switching power converters has always been a main concern. Most times the analysis is based on linear, small signal formalism, in order to tune and then design new schemes. Hence, the scope of the work is motivated by a need of new tools and techniques in order to explore better solutions.

Since dc-dc converters are nonlinear time variant systems, they represent a hard task for control design. As dc-dc converters are variable structured in nature, so nonlinear controllers are proved to be effective for the control of dc-dc converters. These controllers respond immediately to the transient conditions. The types of non-linear controllers include hysteretic controllers, sliding-mode/boundary controllers, etc. Advantages of hysteretic control technique include simplicity in design and do not require feedback loop compensation circuitry. SM controllers are well known for robustness and stability. SM control with infinite operation frequency challenges the feasibility of applying SM controllers to switching power converters. Extreme high switching frequency results in serious EMI, switching losses. Therefore the constant frequency operation becomes the key point to be considered for practical controller design of switching converter.

The buck converter is the most widely used dc-dc converter topology in power management and microprocessor voltage regulator applications. Here the analysis and design of controller is made on the simplest dc-dc converter circuit i.e. the buck converter circuit. The main objective of this research work is to study different control methods and to design an efficient controller with improved performance. The proposed technique requires less component and simple for implementation and eliminates the problem of variable switching frequency.

1.6 Organization of Thesis

The contents of each chapter are organized as follows:

Chapter 1: The importance of switch mode dc-dc converter for various applications is given. This chapter explains the various types of linear and nonlinear control techniques. The problems associated with the control methods for dc-to-dc converters are discussed. A literature survey in detail is done on the control techniques available. The basic principle of SM control theory is described.

Chapter 2: In this chapter the most commonly used analog PWM control method for dc-dc buck converter are studied. Also the sliding mode control technique for buck converter is analyzed, and comparative studies of the discussed control methods are given. The advantage of using sliding-mode controller is discussed. The result shows that SM controller offers better steady state and transient response than other control methods.

Chapter 3: This chapter describes a simple and brief study on hysteretic controllers. The hysteretic control converters are inherently fast response and simple in design. Therefore, the use of hysteretic controller for buck converter is given. This chapter also discusses about the operation of tri-state buck converter. The design of a fixed frequency hysteretic controller for tri-state buck converter is given. The concept of sliding mode control theory is used to study the behavior this control scheme. Simulation results demonstrating the steady state and dynamic performances are presented.

Chapter 4: Includes the thesis conclusions and further research directions.

Chapter 2

CHAPTER 2

Control Methods for dc-dc converter

2.1 Introduction

The switching converters convert one level of electrical voltage into another level by switching action. They are popular because of their smaller size and efficiency compared to the linear regulators. Dc-dc converters have a very large application area. These are used extensively in personal computers, computer peripherals, and adapters of consumer electronic devices to provide dc voltages. The wide variety of circuit topology ranges from single transistor buck, boost and buck-boost converters to complex configurations comprising two or four devices and employing soft-switching or resonant techniques to control the switching losses.

There are some different methods of classifying dc-dc converters. One of them depends on the isolation property of the primary and secondary portion. The isolation is usually made by a transformer, which has a primary portion at input side and a secondary at output side. Feedback of the control loop is made by another smaller transformer or optically by optocoupler. Therefore, output is electrically isolated from input. This type includes Fly-back dc-dc converters and PC power supply with an additional ac-dc bridge rectifier in front. However, in portable devices, since the area to implement this bulky transformer and other off-chip components is very big and costly, so non-isolation dc-dc converters are more preferred.

The non-isolated dc/dc converters can be classified as follows:

- Buck converter (step down dc-dc converter),
- Boost converter (step up dc-dc converter),
- Buck-Boost converter (step up-down dc-dc converter, opposite polarity), and
- Cuk converter (step up-down dc-dc converter).

Similar type of methods for analysis and control are applied to many of these converters. The dc-dc buck converter is the simplest power converter circuit used for many power management and voltage regulator applications. Hence, the analysis and design of the control structure is done for the buck converter circuit. All the terms, designs, figures, equations and discussions in this thesis are most concerned with dc-dc buck converter circuit.

2.2 The Dc-dc Buck Converter

The buck converter circuit converts a higher dc input voltage to lower dc output voltage. The basic buck dc-dc converter topology is shown in figure. 2.1. It consists of a controlled switch S_w , an uncontrolled switch D (diode), an inductor L , a capacitor C , and a load resistance R .

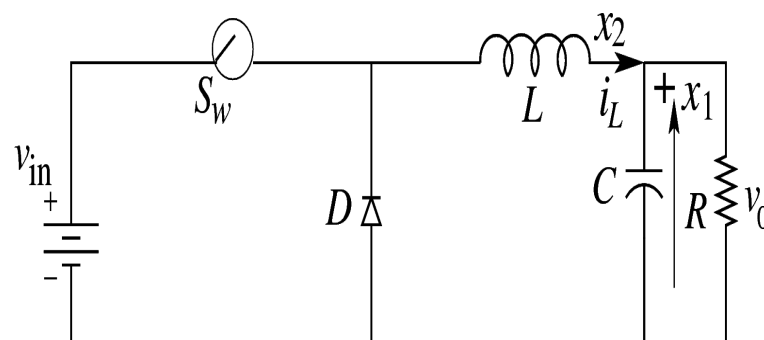


Figure 2.1: Dc-dc buck converter topology

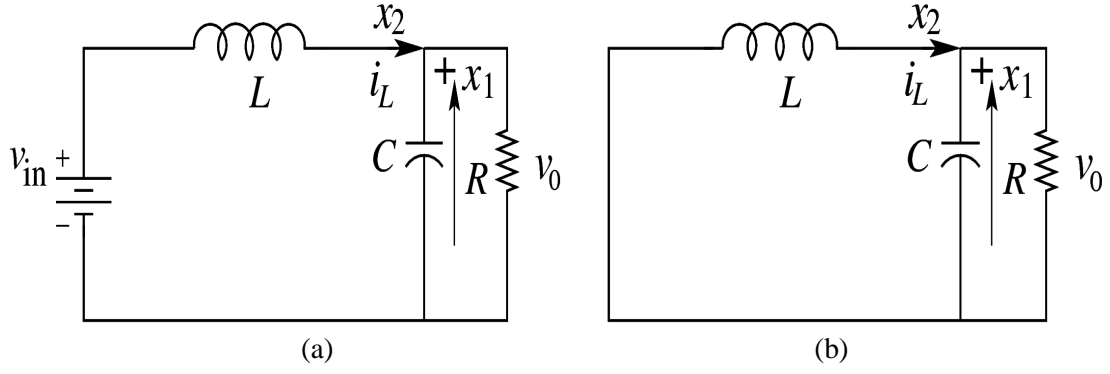


Figure 2.2: Buck converter circuit when switch: (a) turns on (b) turns off

In the description of converter operation, it is assumed that all the components are ideal and also the converter operates in CCM. In CCM operation, the inductor current flows continuously over one switching period. The switch is either on or off according to the switching function q and this results in two circuit states. The first sub-circuit state is when the switch is turned on, diode is reverse biased and inductor current flows through the switch, which can be shown in figure 2.2(a). The second sub-circuit state is when the switch is turned off and current freewheels through the diode, which is shown figure 2.2(b).

When the switch S_1 is on and D is reverse biased, the dynamics of inductor current i_L and the capacitor voltage v_C are

$$\frac{di_L}{dt} = \frac{1}{L} v_{in} - v_0 \quad \text{and} \quad \frac{dv_0}{dt} = \frac{dv_C}{dt} = \frac{1}{C} i_C \quad (2.1)$$

When the switch S_1 is off and D is forward biased, the dynamics of the circuit are

$$\frac{di_L}{dt} = -\frac{1}{L} v_0 \quad \text{and} \quad \frac{dv_0}{dt} = \frac{dv_C}{dt} = \frac{1}{C} i_C \quad (2.2)$$

When switch S_1 is off and D is also not conducting,

$$\frac{di_L}{dt} = 0 \quad \text{and} \quad \frac{dv_0}{dt} = \frac{dv_C}{dt} = \frac{1}{C} i_C \quad (2.3)$$

The state space representation for converter circuit configuration can be expressed as

$$\frac{dx}{dt} = \begin{cases} A_1x + B_1U; & \text{when } S \text{ is closed,} \\ A_2x + B_2U; & \text{when } S \text{ is opened.} \end{cases} \quad (2.4)$$

where $x = [x_1 \ x_2]^T = [v_C \ i_L]^T$ is the state vector and A's and B's are the system matrices.

The state matrices and the input vectors for the ON and OFF periods are

$$A_1=A_2 = \begin{bmatrix} -\frac{1}{RC} & \frac{1}{C} \\ -\frac{1}{L} & 0 \end{bmatrix}, \quad B_1 = \begin{bmatrix} 0 \\ \frac{1}{L} \end{bmatrix}, \quad B_2 = \begin{bmatrix} 0 \\ 0 \end{bmatrix}$$

$$\text{and } U = \begin{bmatrix} V_{in} \\ 0 \end{bmatrix}.$$

2.3 Modes of Operation

The operation of dc-dc converters can be classified by the continuity of inductor current flow. So dc-dc converter has two different modes of operation that are (a) Continuous conduction mode (CCM) and (b) Discontinuous conduction mode (DCM). A converter can be design in any mode of operation according to the requirement.

2.3.1 Continuous Conduction Mode

When the inductor current flow is continuous of charge and discharge during a switching period, it is called Continuous Conduction Mode (CCM) of operation shown in figure 2.3(a). The converter operating in CCM delivers larger current than in DCM. In CCM, each switching cycle T_s consists of two parts that is D_1T_s and D_2T_s ($D_1 + D_2 = 1$). During D_1T_s , inductor current increases linearly and then in D_2T_s it ramps down that is decreases linearly.

2.3.2 Discontinuous Conduction Mode

When the inductor current has an interval of time staying at zero with no charge and discharge then it is said to be working in Discontinuous Conduction Mode (DCM) operation and the waveform of inductor current is illustrated in figure 2.3(c). At lighter load currents, converter operates in DCM. The regulated output voltage in DCM does not have a linear relationship with the input voltage as in CCM. In DCM, each switching cycle is divided into of three parts that is D_1T_s , D_2T_s and D_3T_s ($D_1 + D_2 + D_3 = 1$). During the third mode i.e. in D_3T_s , inductor current stays at zero.

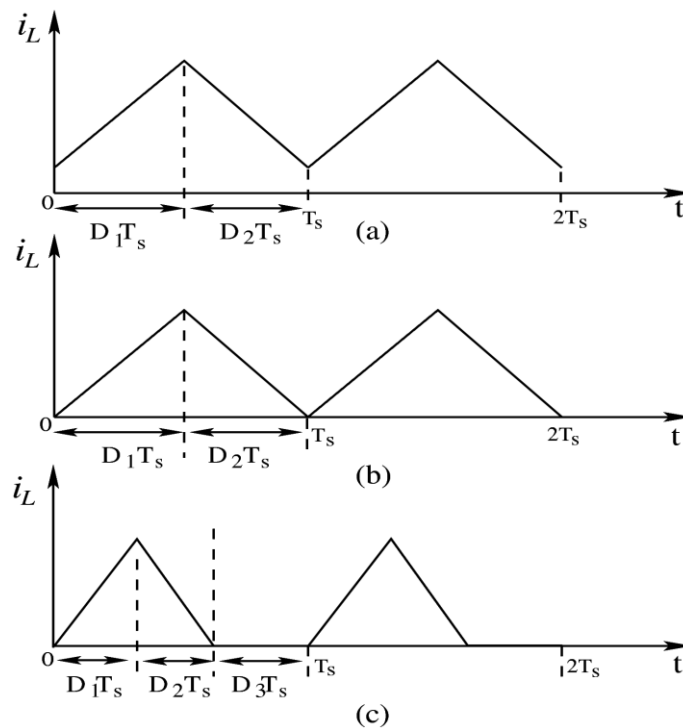


Figure 2.3: Inductor current waveform of PWM converter (a) CCM (b) boundary of CCM and DCM (c) DCM

2.4 Control Methods for Dc-dc Buck Converter

Voltage-mode control and Current-mode control are two commonly used control schemes to regulate the output voltage of dc-dc converters. Both control schemes have been widely used in low-voltage low-power switch-mode dc-dc converters integrated circuit design in industry. Feedback loop method automatically maintains a precise output voltage regardless of variation in input voltage and load conditions.

2.4.1 Voltage-mode Controlled Buck Converter

The voltage feedback arrangement is known as voltage-mode control when applied to dc-dc converters. Voltage-mode control (VMC) is widely used because it is easy to design and implement, and has good immunity to disturbances at the references input. VMC only contains single feedback loop from the output voltage.

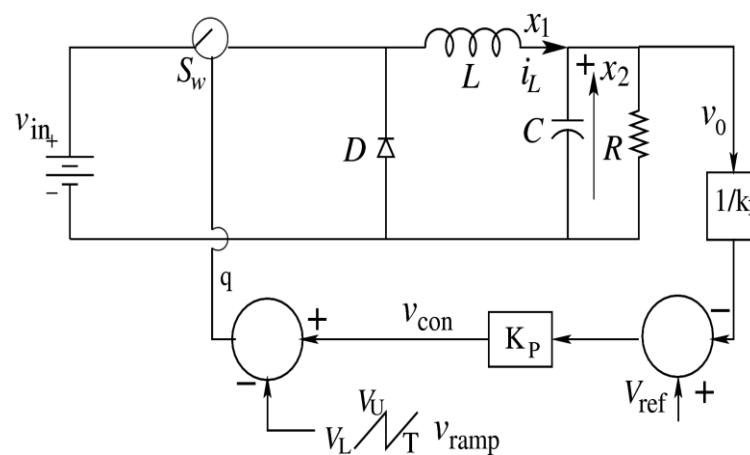


Figure 2.4: Block diagram of voltage mode controller

The voltage mode controlled buck converter circuit is shown in figure 2.4. It consists of a controlled switch S_w (MOSFET), an uncontrolled switch diode D (diode), an inductor L , a capacitor C , and a load resistance R . The circuit shown in figure 2.4 is a nonsmooth dynamical system described by two sets of differential equations:

$$\frac{di_L}{dt} = \begin{cases} \frac{v_{in} - v_0}{L}, & S_w \text{ is conducting} \\ \frac{-v_0}{L}, & S_w \text{ is blocking} \end{cases} \quad (2.5)$$

$$\text{and} \quad \frac{dv_0}{dt} = \frac{i_L - \frac{v_0}{R}}{C} \quad (2.6)$$

The switch is controlled by analog PWM feedback logic. This is achieved by obtaining a control voltage v_{con} as function of the output capacitor voltage v_c and a reference signal V_{ref} in the form,

$$v_{con} = k_p \left(V_{ref} - \frac{v_0}{k_1} \right) \quad (2.7)$$

where, k_p is the gain of proportional controller and k_1 is the factor of reduction of the output voltage v_0 . An externally generated saw-tooth voltage defined as $v_{ramp}(t)$ is used to determine the switching instants.

$$v_{ramp}(t) = V_L + (V_U - V_L)F(t/T_s) \quad (2.8)$$

Where T_s is the time period and V_U and V_L are upper and lower threshold voltages respectively. Here $F(x)$ denotes the fractional part of x : $F(x) = x \bmod 1$. In voltage mode control, the controlled voltage v_{con} is then compared with the periodic saw-tooth wave V_{ramp} , to generate the switching signal $q \in [1,0]$ is described by

$$\begin{aligned} \text{If } V_{ramp} < v_{con}; & \quad q = 1 \\ \text{If } V_{ramp} > v_{con}; & \quad q = 0 \end{aligned} \quad (2.9)$$

The inductor current increases while the switch S_w is on i.e. $q = 1$ and falls while the switch S is off i.e. $q = 0$.

If the current reaches zero value before the next clock cycle, the operation is said to be in DCM, else it is in CCM. The state equation that describes the dynamics of the buck converter can be written as

$$\frac{dx}{dt} = \begin{cases} A_1 x + B_1 U; & (k_p x_1 - V_{ref}) < V_{ramp}, \\ A_2 x + B_2 U; & (k_p x_1 - V_{ref}) > V_{ramp}. \end{cases} \quad (2.10)$$

where $x = [x_1 \ x_2]^T = [v \ i]^T$ is the state vector and A's and B's are the system matrices.

The state matrices and the input vectors of the converter are given by

$$A_1 = A_2 = \begin{bmatrix} -\frac{1}{RC} & \frac{1}{C} \\ -\frac{1}{L} & 0 \end{bmatrix}, \quad B_1 = \begin{bmatrix} 0 \\ \frac{1}{L} \end{bmatrix}, \quad B_2 = \begin{bmatrix} 0 \\ 0 \end{bmatrix}$$

$$\text{and } U = V_{in} \ 0$$

The switching hypersurface (h) can be written as

$$h = x_1 - V_{ref} - \frac{V_{ramp}}{k_p} = 0, \quad k_p \neq 0. \quad (2.11)$$

For discontinuous conduction mode, inductor current reaches zero before the next clock cycle. In this case, the state equation of the converter can be written as

$$\begin{bmatrix} \dot{x}_1 \\ \dot{x}_2 \end{bmatrix} = \begin{bmatrix} -\frac{1}{RC} & 0 \\ 0 & 0 \end{bmatrix} \begin{bmatrix} x_1 \\ x_2 \end{bmatrix} \quad (2.12)$$

However, VMC have a few disadvantages. Any change in input voltage will alter the gain and influence the system dynamics behavior. VMC cannot correct any disturbance immediately until it is detected at the output since the disturbances are delayed in phase by the inductor and capacitor prior to the output.

2.4.2 Current-mode Controlled Buck Converter

Another control scheme that is widely used for dc-dc converters is current mode control. Current-mode controlled dc-dc converters usually have two feedback loops: a current feedback loop and a voltage feedback loop. The inductor current is used as a feedback state.

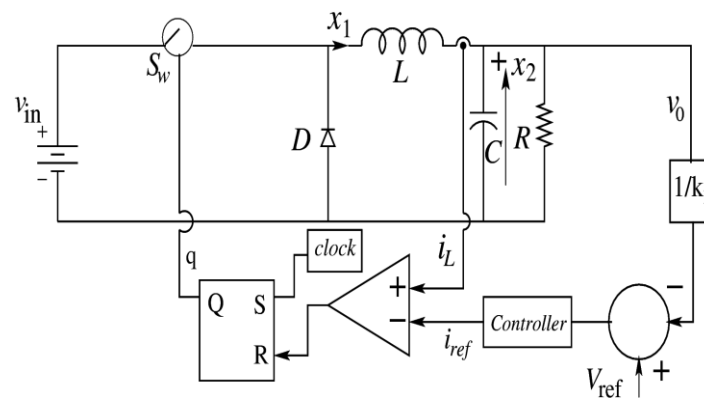


Figure 2.5: Current-mode controlled dc-dc buck converter

A current mode controlled dc-dc buck converter circuit is shown in figure.2.5. At the beginning of a switching cycle, the clock signal sets the flip-flop ($q = 1$), turning on the (MOSFET) switch. The switch current, which is equal to the inductor current during this interval, increases linearly. The inductor current i_L is compared with the control signal i_{ref} from the controller. When i_L is slightly greater than i_{ref} , the output of the comparator goes high and resets the flip-flop ($q = 0$), thereby turning off the switch. The switch will be turned on again by the next clock signal and the same process repeated.

The buck converter circuit operates at continuous conduction mode. Depending on the state of the switch, there are two circuit configurations, which are described by the following differential equations:

$$\frac{di_L}{dt} = \begin{cases} \frac{v_{in} - v_0}{L}, & S_w \text{ is conducting} \\ \frac{-v_0}{L}, & S_w \text{ is blocking} \end{cases} \quad (2.13)$$

and

$$\frac{dv_0}{dt} = \frac{i_L - \frac{v_0}{R}}{C} \quad (2.14)$$

If the switch position is expressed with the switching function q , then

$$q = \begin{cases} 1, & S_w \text{ closed} \\ 0, & S_w \text{ opened} \end{cases} \quad (2.15)$$

The control input signal is proportional to reference current i_{ref} . The reference current i_{ref} is a function of output of the controller to regulate the output voltage.

The control voltage can be defined as,

$$v_{con} = k_p \left(V_{ref} - \frac{v_0}{k_1} \right) \text{ for P controller}$$

and

$$v_{con} = k_p \left(V_{ref} - \frac{v_0}{k_1} \right) + k_I \int \left(V_{ref} - \frac{v_0}{k_1} \right) dt, \text{ for PI controller.}$$

Hence the reference current can be written as $i_{ref} = \frac{v_{con}}{R_f}$, where R_f is a proportionality factor. The voltage waveforms are scaled to equivalent current waveforms by the proportionality factor R_f .

The state equation that describes the dynamics of the buck converter can be written as

$$\frac{dx}{dt} = \begin{cases} A_1 x + B_1 U; & \text{when } S \text{ is closed,} \\ A_2 x + B_2 U; & \text{when } S \text{ is opened.} \end{cases} \quad (2.16)$$

where $x = [x_1 \ x_2]^T = [v \ i]^T$ is the state vector and A's and B's are the system matrices.

The state matrices and the input vectors for the ON and OFF periods are

$$A_1=A_2 = \begin{bmatrix} -\frac{1}{RC} & \frac{1}{C} \\ -\frac{1}{L} & 0 \end{bmatrix}, \quad B_1 = \begin{bmatrix} 0 \\ \frac{1}{L} \end{bmatrix}, \quad B_2 = \begin{bmatrix} 0 \\ 0 \end{bmatrix}$$

and $U = v_{in} \ 0$.

There are two types of current mode control strategies. In both, the switch is turned on at the beginning of every clock period. In peak current mode control, the inductor current is compared with a reference current signal with a compensation ramp, and the switch is turned off when the two become equal. In the average current mode control, the inductor current is compared with a ramp waveform, and the switch is turned off when $i_L < i_{rmp}$. It is turned on again at the next clock instant. Here a brief overview of peak current mode control scheme is described.

2.4.2.1 Current Mode Control with Compensating Ramp

Figure 2.7 shows the waveform of inductor current of a switching converter operating in continuous conduction mode (CCM). The inductor current changes with a slope m_1 during the first subinterval, and a slope $-m_2$ during the second subinterval. The peak inductor current is controlled and the controlled method is therefore called peak current-mode control. The current mode controller is unstable whenever the steady-state duty cycle is greater than 0.5, resulting in sub-harmonic oscillation.

To avoid this stability problem, the control scheme is usually modified by adding an external ramp to the sensed inductor current waveform. Let the slope of compensating ramp is m_a . when $m_a \geq 0.5m_2$, then the controller is stable for all duty cycles. The relationship between the ramp, inductor and reference current is given in (2.12),

$$i_a \ dT_S + i_L \ dT_S = i_{ref} \tag{2.17}$$

Then, the control equation is given by

$$i_L - \left(i_{ref} - m_a \frac{t}{T_S} \right) = 0 \quad (2.18)$$

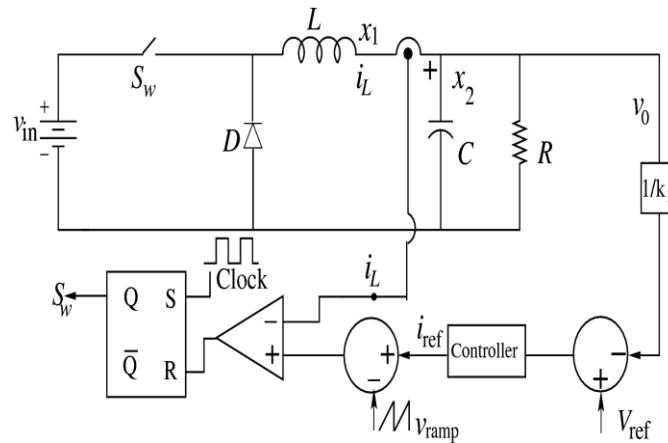


Figure 2.6: Peak Current Mode Control

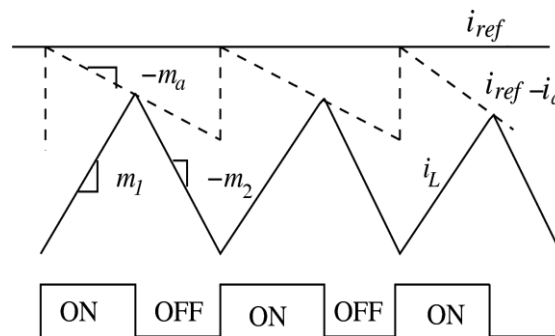


Figure 2.7: Inductor Current waveform with compensating ramp

Advantages of peak current mode control include Control of the peak inductor current, inherent peak current limiting and sharing, good dynamic performance, first order transfer function. Some of the main drawbacks of this control are the limited duty ratio, increased output impedance, sub-harmonic oscillation, noise sensitivity. These problems are rectified by means of an artificial ramp signal either subtracted from the control signal or added to the inductor-current signal.

2.5 Sliding Mode Control for Dc-dc Buck Converter

Buck Converter is a time variable and a nonlinear switch circuit which possesses variable structure features. Sliding mode control is well known for its good dynamic response and stability due to its insensitive for parameters change and easier in implementation, so this control technique is used extensively for the control of dc-dc power converters [40], [41], [46]. This section explains about the implementation of a hysteresis modulation (HM) based SM controller for dc-dc buck converter.

2.5.1 System Modeling

A typical SM controller for switching power converters has two control modes: voltage mode and current mode. Here, voltage mode control is employed, i.e. output voltage v_0 , is the parameter to be controlled. Figure 2.8 shows the schematic diagram of a SM voltage controlled buck converter. Here the state space description of the buck converter under SM voltage control, where the control parameters are the output voltage error and the voltage error dynamics is described.

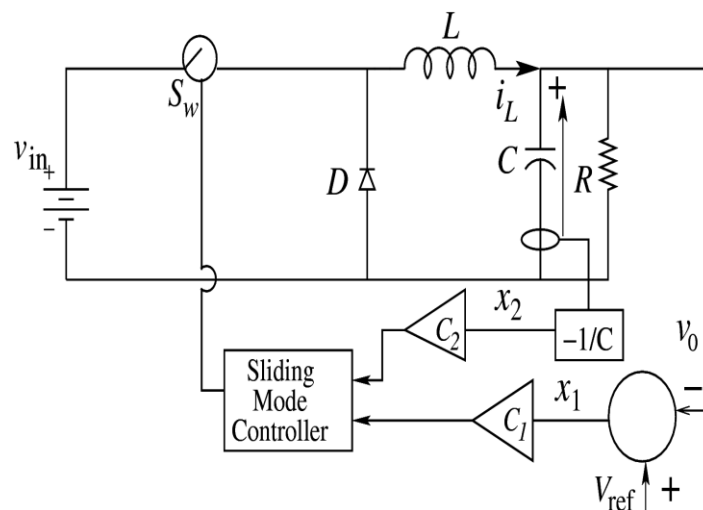


Figure 2.8: Basic structure of an SMC buck converter system

Hence the voltage error x_1 and the voltage error dynamics (i.e. the rate of change of voltage error) x_2 under CCM operation can be expressed as

$$x = \begin{bmatrix} x_1 \\ x_2 \end{bmatrix} = \begin{bmatrix} V_{ref} - v_0 \\ \frac{d}{dt}(V_{ref} - v_0) \end{bmatrix}$$

i.e.
$$\begin{cases} x_1 = V_{ref} - v_0 \\ x_2 = \frac{dx_1}{dt} = -\frac{dv_0}{dt} = -\frac{i_c}{C} \end{cases} \quad (2.19)$$

where V_{ref} represents the reference voltage, v_0 is the output voltage, and i_c denotes the capacitor current. Here the reference voltage V_{ref} is assumed to be constant and capacitor ESR is zero. Then, by differentiating (4) with respect to time

$$\begin{aligned} \dot{x}_1 &= x_2 \\ \dot{x}_2 &= -\frac{1}{C} \frac{d}{dt} i_c \end{aligned} \quad (2.20)$$

The capacitor current equation when the switch is on can be expressed as

$$i_c = i_L - i_0 \quad (2.21)$$

Substituting equation (2.18) into (2.19) results in

$$\dot{x}_2 = -\frac{1}{C} \left[\frac{d}{dt} i_L - \frac{d}{dt} i_0 \right] \quad (2.22)$$

Consider dc-dc buck converter equation when the switch is on

$$\frac{d}{dt} i_L = \frac{v_{in} - v_0}{L} \quad (2.23)$$

Substituting (2.21) into (2.20) and for $i_0 = \frac{v_0}{R}$ results in

$$\dot{x}_2 = -\frac{1}{C} \left[\frac{v_{in} - v_0}{L} - \frac{d}{dt} \frac{v_0}{R} \right] \quad (2.24)$$

By rearranging the terms, we get
$$\dot{x}_2 = -\frac{v_{in}}{LC} + \frac{v_0}{LC} + \frac{1}{RC} \frac{dv_0}{dt} \quad (2.25)$$

From equation (2.19), the output voltage, $v_0 = V_{ref} - x_1$ (2.26)

Substituting equation (2.24) into (2.23) leads to

$$\dot{x}_2 = -\frac{x_1}{LC} - \frac{x_2}{RC} - \frac{v_{in}}{LC} + \frac{V_{ref}}{LC} \quad (2.27)$$

Hence, the system equations, in terms of state variables x_1 and x_2 can be written as

$$\begin{cases} \dot{x}_1 = x_2 \\ \dot{x}_2 = -\frac{x_1}{LC} - \frac{x_2}{RC} - \frac{v_{in}}{LC} + \frac{V_{ref}}{LC} \end{cases} \quad (2.28)$$

The state space model describing the system can be derived as

$$\begin{aligned} \dot{x} &= Ax + Bu + D \quad (2.29) \\ A &= \begin{bmatrix} 0 & 1 \\ -\frac{1}{LC} & -\frac{1}{RC} \end{bmatrix}, \quad B = \begin{bmatrix} 0 \\ -\frac{v_{in}}{LC} \end{bmatrix}, \quad D = \begin{bmatrix} 0 \\ \frac{V_{ref}}{LC} \end{bmatrix} \end{aligned}$$

For DCM, inductor current is zero before the next clock cycle. This creates constraints to the state variables. This can be derived by putting, $i_L = 0$. Hence, the equation of the can be written as

$$x_2 = \frac{1}{RC} [V_{ref} - x_1] \quad (2.30)$$

The equation 2.12 represents a straight line in phase plane passing through points $(V_{ref}, 0)$ and $(0, V_{ref}/RC)$.

2.5.2 Design of SM Controller

In SM controller, the controller employs a sliding surface to decide its input states to the system. For SM controller, the switching states u which corresponds the turning on and off of the converter' switch is decided by sliding line. The sliding surface is described as a linear combination of the state variables. Thus the switching function is chosen as

$$S = c_1x_1 + c_2x_2 = C^T x = 0 \quad (2.31)$$

where $C^T = [c_1, c_2]$ is the vector of sliding surface coefficients and $x = [x_1 \ x_2]^T$. This equation describes a sliding line in the phase plane passing through the origin, which represents the stable operating point for this converter (zero output voltage error and its derivative).

The sliding line acts as a boundary that splits the phase plane into two regions. Each of this region is specified with a switching state to direct the phase trajectory toward the sliding line. When the phase trajectory reaches and tracks the sliding line towards the origin, then the system is considered to be stable, i.e., $\dot{x}_1 = 0$ and $\dot{x}_2 = 0$.

Substituting equation (2.20) into (2.31) results in

$$S = c_1x_1 + c_2\dot{x}_1 = 0 \quad (2.32)$$

This describes the system dynamic in sliding mode. Thus, if existence and reaching conditions of the sliding mode are satisfied, a stable system is obtained.

To ensure that a system follows its sliding surface, a control law is proposed. In this system, the control law is defined as

$$u = \begin{cases} 1 = \text{ON} & \text{when } S > k \\ 0 = \text{OFF} & \text{when } S < -k \\ \text{previous state,} & \text{otherwise} \end{cases} \quad (2.33)$$

where k is an arbitrarily small value. The reason for choosing $S > k$ and $S < -k$ as the switching boundary is to introduce a hysteresis band which determines the switching frequency of the converter. If the parameters the state variables are such that $S > k$, switch S_w of the buck converter will turn on. When $S < -k$, it will turn off. In the region $-k \leq S \leq k$, switch remains in its previous state.

Thus, this prevents the SM controller from operating at a high frequency for the power switch to respond. It also alleviates the chattering effect which induces extremely high frequency switching. The switching conditions in equation (2.33) are graphically shown in figure 2.9.

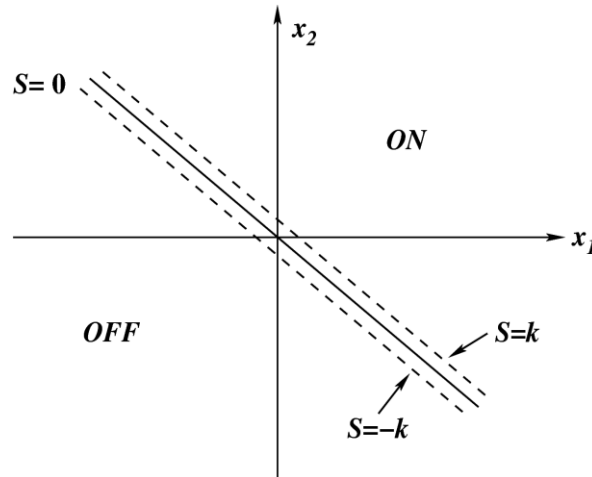


Figure 2.9: Sliding line on $x_1 - x_2$ phase plane

2.5.3 Derivation of SM Existence Condition

The control law in (2.33) only provides the information that the system trajectory is driven toward the sliding line. In order to ensure that the trajectory is maintained on the sliding line, the existence condition of SM operation, which is derived from Lyapunov's second method to determine asymptotic stability, must be satisfied.

$$\lim_{S \rightarrow 0} S \cdot \dot{S} < 0 \quad (2.34)$$

Hence the specific conditions for the sliding regime to exist can also be expressed as

$$\begin{aligned} \dot{S} < 0, & \text{ if } S > 0 \\ \dot{S} > 0, & \text{ if } S < 0 \end{aligned} \quad (2.35)$$

The existence condition can be expressed in the standard form

$$\dot{S} = C^T \dot{x} = C^T (Ax + Bu + D) \quad (2.36)$$

Then the equation (2.32) in two circumstances, it gives,

$$\begin{cases} \dot{S}_{S>0} = C^T \dot{x} \\ \quad = C^T Ax + C^T B + C^T D < 0 \\ \dot{S}_{S<0} = C^T \dot{x} \\ \quad = C^T Ax + C^T D < 0 \end{cases} \quad (2.37)$$

For buck converter, when $S \rightarrow 0^+$, the switch function $q = 1$, and when $S \rightarrow 0^-$, the switch function $q = 0$. By substituting the matrices A, B, and D, and state variable x , the above inequality becomes:

Case-I when $S \rightarrow 0^+$, $\dot{S} < 0$

$$\lambda_1 = \left(c_1 - \frac{c_2}{RC} \right) x_2 - \frac{c_2}{LC} x_1 + \frac{V_{ref} - V_{in}}{LC} c_2 < 0 \quad (2.38)$$

Case-II when $S \rightarrow 0^-$, $\dot{S} > 0$

$$\lambda_2 = \left(c_1 - \frac{c_2}{RC} \right) x_2 - \frac{c_2}{LC} x_1 + \frac{V_{ref}}{LC} c_2 > 0 \quad (2.39)$$

The equations $\lambda_1 = 0$ and $\lambda_2 = 0$ define two lines in the phase plane with the same slope passing through points $V_{ref}, 0$ and $V_{ref} - v_{in}, 0$ respectively. These two lines determine the two boundaries of existence region from simulation these are clearly shown in figure 2.10. Point $V_{ref} - v_{in}, 0$ is the stable equilibrium point for the trajectories when the switch is on. Similarly the trajectories corresponding to the system off state dynamic always tries to converge to the point $V_{ref}, 0$, which is the off state equilibrium point. The phase trajectory in SM operation is shown in figure 2.11. Sliding mode will occur on the portion of the sliding line, $S = 0$, that covers both the on state and off state region and it will overshoot the sliding line if the phase trajectory present outside the existence region. The value of system parameters and sliding coefficients are given in section 2.6. In figure

2.12, we have increased the value of sliding coefficients c_1 to 5, so the overshoot is increased and that changes the structure of the trajectory.

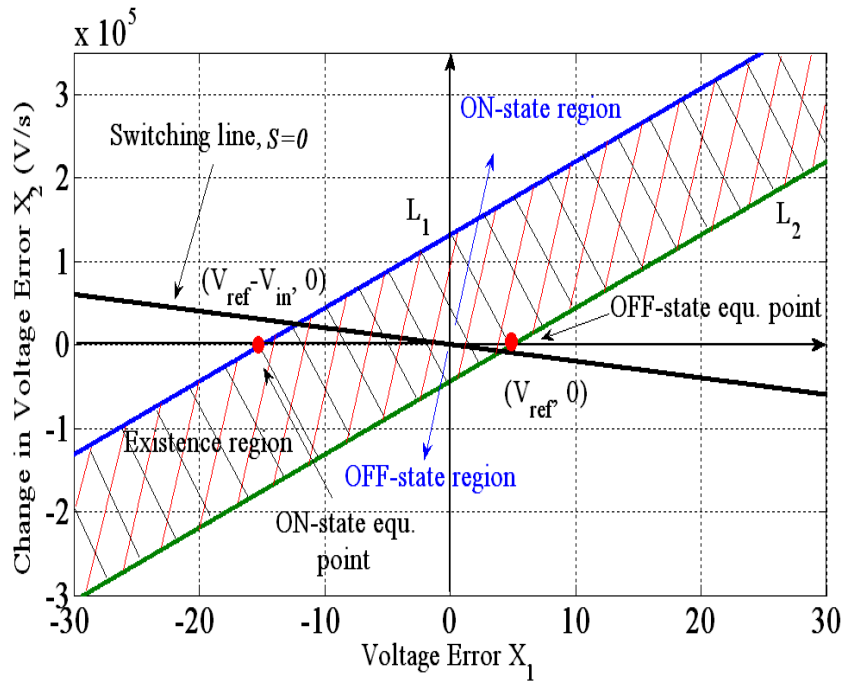


Figure 2.10: Region of existence of SM mapped in the phase plane

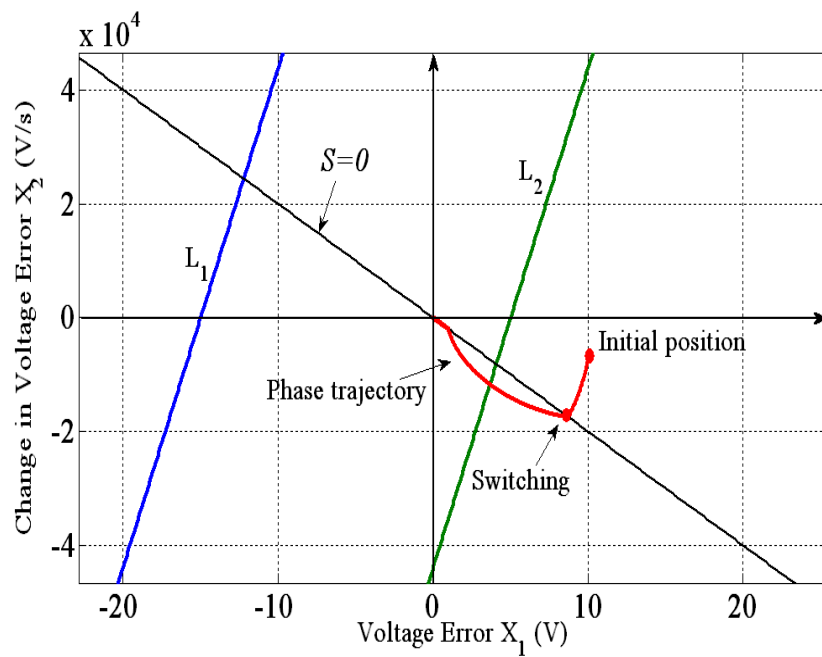


Figure 2.11: Evolution of phase trajectory in phase plane for $c_1 > c_2/RC$

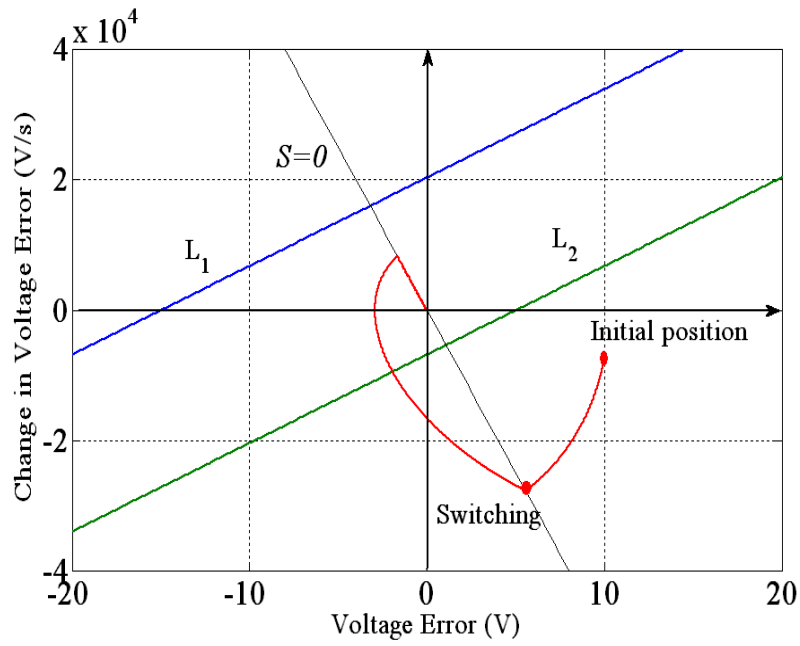


Figure 2.12: Phase plane diagram for $c_1 > c_2/RC$

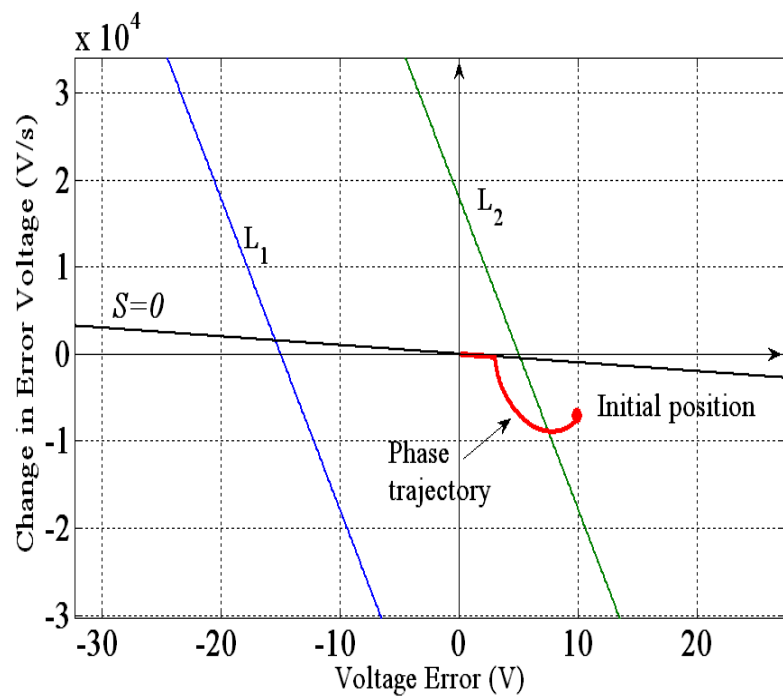


Figure 2.13: Phase plane diagram for $c_1 < c_2/RC$

The chattering phenomenon can be defined as an undesirable oscillation around the sliding surface at a high switching frequency due to the presence of switching imperfections, parasitic effects etc. To control this undesirable high frequency oscillation, generally a hysteresis band is imposed and the width hysteresis band determines the switching frequency. The chattering phenomenon is illustrated in figure 2.14. From figure, it is seen that narrower the hysteresis band higher the switching frequency and except steady state operation, switching frequency is not constant.

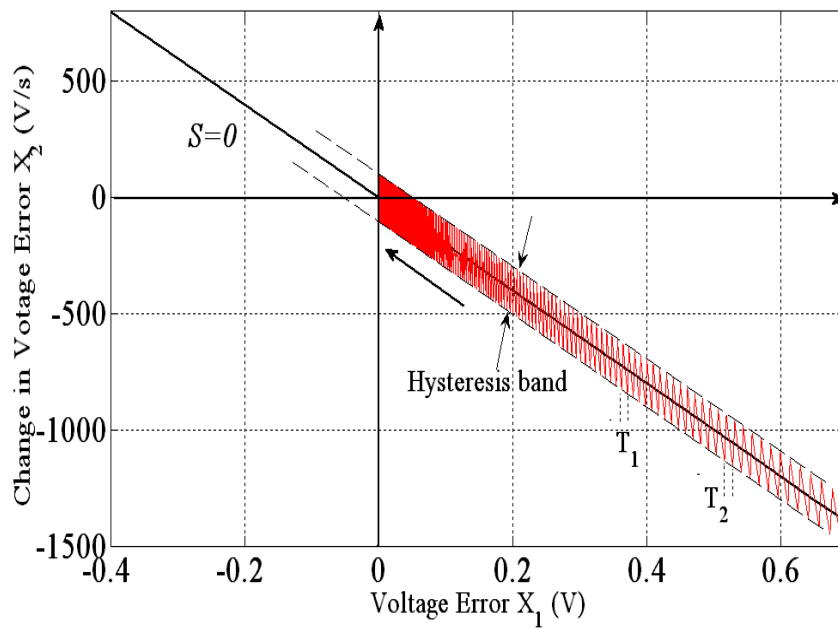


Figure 2.14: Chattering Phenomena of SM control

2.6 Simulation Results and Discussions

In this section the simulation results are presented for comparison between the different control methods that are discussed in above sections undergoing load current step transient, input voltage step transient. The results of comparison are explained. There are two different types of comparison study are presented. The first one is the performance comparison between PWM based voltage-mode controlled buck converter and HM based SM controlled buck converter. The second one is the performance comparison between peak current-mode controlled buck converter with HM based SM controlled buck converter.

The control methods have the same power circuit parameters and operate at the same input and output voltages. The design specifications and the circuit parameters, for simulation are chosen as: input voltage $v_{in}=20V$, desired output voltage $v_0=5V$, inductance $L=3mH$, capacitance $C=69\mu F$, and minimum load resistance $R_{min}=10\Omega$, maximum load resistance $R_{max}=15\Omega$, voltage reduction factor $k_1=0.4$, proportional gain $k_p=2$, and the upper and lower threshold of ramp voltage $V_L=3.8$ and $V_U=8.2$. The sliding coefficients $c_1=2$ and $c_2=0.001$. The switching frequency f_s is set to 100 kHz.

2.5.1 PWM based Voltage-Mode Controller versus SM Controller

In this subsection, dynamic performance of PWM based voltage mode controlled buck converter is compared with HM based SM controlled buck converter. The results from simulation are given in figure 2.15-2.18. The transient responses of buck converter employing PWM based voltage-mode control and SM control techniques are shown in following figures respectively.

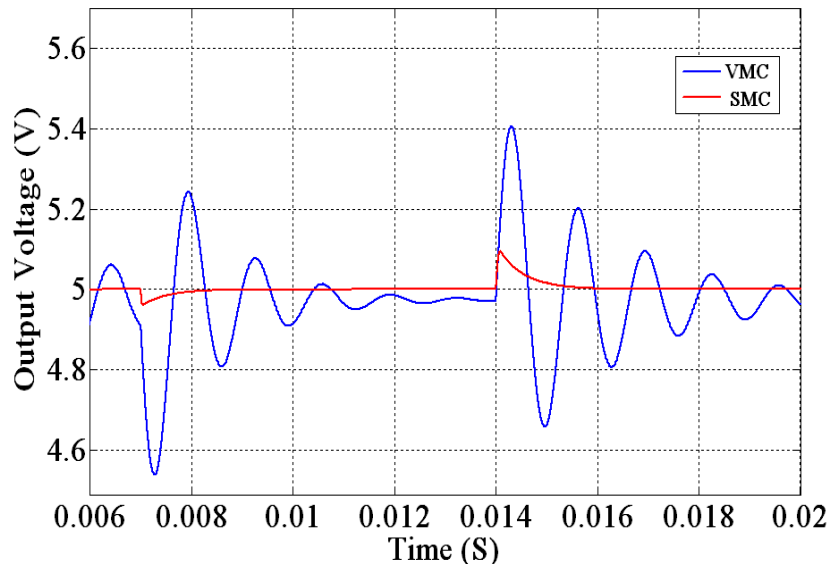


Figure 2.15: Output voltage response due to a step change in load resistance from 15Ω to 10Ω back to 15Ω

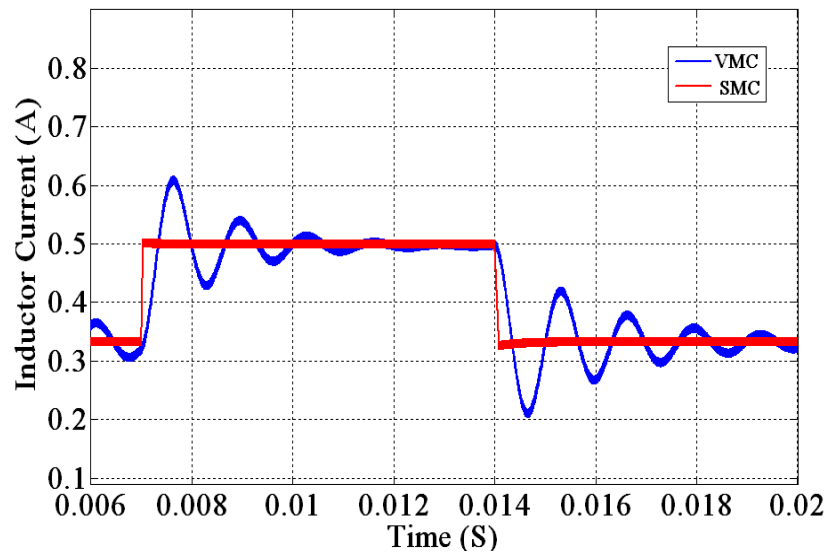


Figure 2.16: Inductor Current response due to a step change in load resistance from 15Ω to 10Ω and back to 15Ω

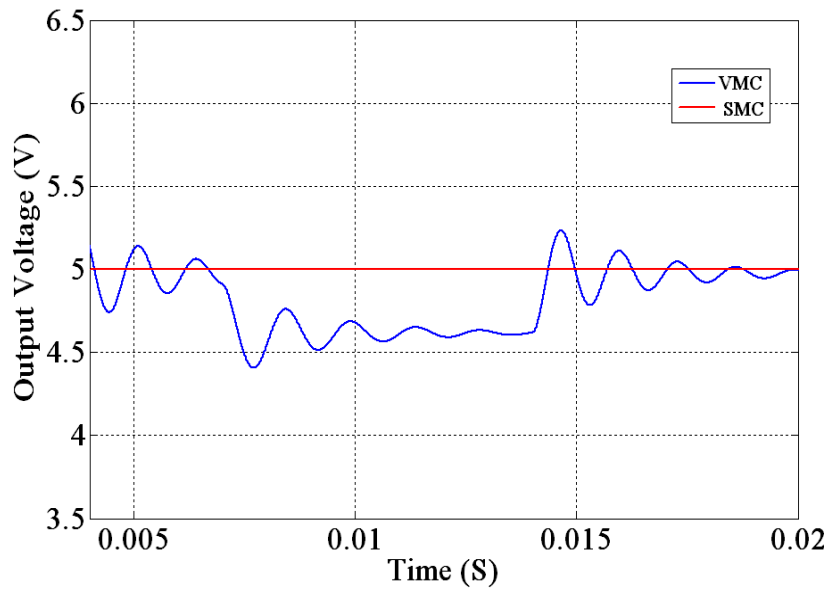


Figure 2.17: Output Voltage response for a change in input voltage from 20V to 15V and back to 20V

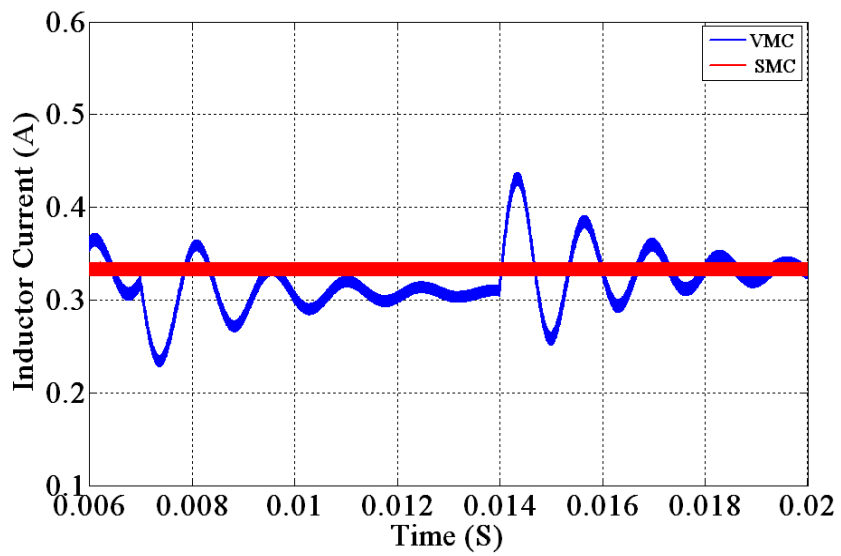


Figure 2.18: Inductor Current response for a change in input voltage from 20V to 15V and back to 20V

Figure 2.15 shows the output voltage waveform of the converter for a step change in load resistance from 15Ω to 10Ω and then back to 15Ω for both VMC and SM control. The SM control Scheme takes 1.2ms settling time (time required to return to the steady state) with an overshoot of 0.04volt as compared to 7ms and 0.5volt in case of the VMC. Hence, SM control has a smaller overshoot and zero steady state error than VMC.

The inductor current response for a step load transient from 15Ω to 10Ω and then back to 15Ω for both VMC and SM control is then shown figure 2.16. From the result in figure 2.16, we can see that the settling time is 0.04ms which is less compared to VMC that has 7ms. This shows poor large-signal transient response due to the oscillatory nature of the output voltage and the long settling time.

Similarly the system response for a change in input voltage from 20 volt to 15 volt then back to 20 volt using both control schemes is shown in figure 2.17 and figure 2.18 respectively. From the results it is shown that the output of converter is not affected by the input voltage variation in case of SM control where as the performance of converter with VMC degrades having a long settling time and larger steady state error. This demonstrates the advantage SM controller over VMC for providing faster transient response for a wide operating range.

2.5.2 Peak-Current-Mode Controller versus SM Controller

In this subsection, the dynamic performance of Peak-Current-mode controlled buck converter is compared with HM based SM controlled buck converter. The comparison results are shown in the following figures. The transient responses of buck converter employing PWM based peak-current-mode control and SM control techniques are shown in the following figures respectively.

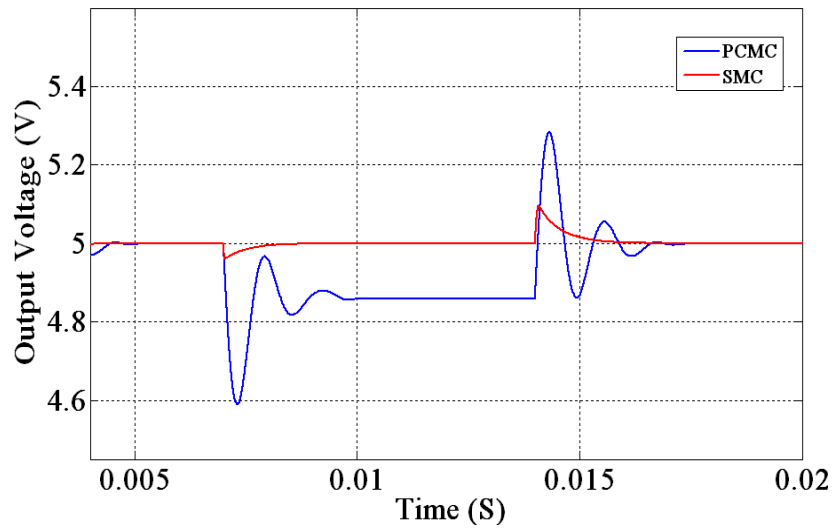


Figure 2.19: Output Voltage response with step load transient from 15Ω to 10Ω and then back to 15Ω

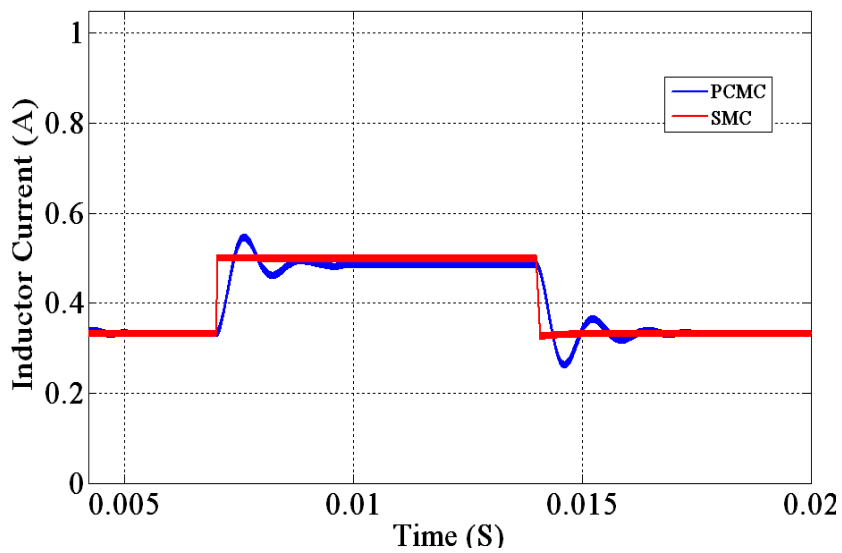


Figure 2.20: Inductor Current response with step load transient from 15Ω to 10Ω and then back to 15Ω

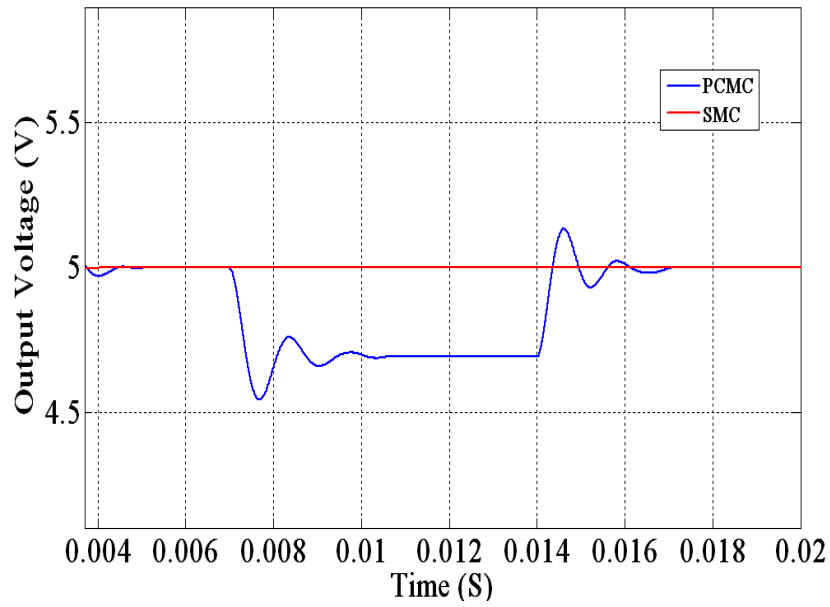


Figure 2.21: Output Voltage response for a change in input voltage from 20V to 15V and back to 20V

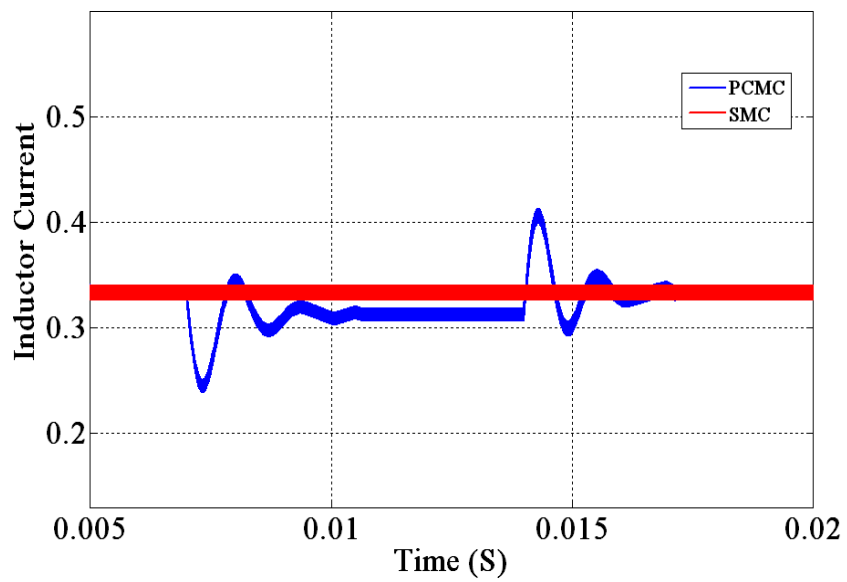


Figure 2.22: Inductor Current response for a change in input voltage from 20V to 15V and back to 20V

From the above figures (figure 2.19 to figure 2.22), it is seen that the transient response corresponding to SM controller is faster and has smaller overshoot when compared to the transient responses in PCMC. PCMC is usually faster than VMC because of its additional inner current control loop and compensation technique used for PCMC is lesser complex than VMC. Also the transient response of PCMC is faster than VMC. But, when the PCMC method is compared with the SM controller, again SM control method is proved to be better solution for its robustness to line and load variations.

The transient response of SM controlled buck converter can be understood from phase plane analysis method. The phase plane plot of SM control for a step change in load from 15Ω to 10Ω and then back to 15Ω is shown in figure 2.23. From figure we can see that the phase trajectory starting from any initial position always tries to settle at the stable equilibrium point (origin) and when the load changes the trajectory located at some other initial position again tracks the sliding line by reaching back to origin.

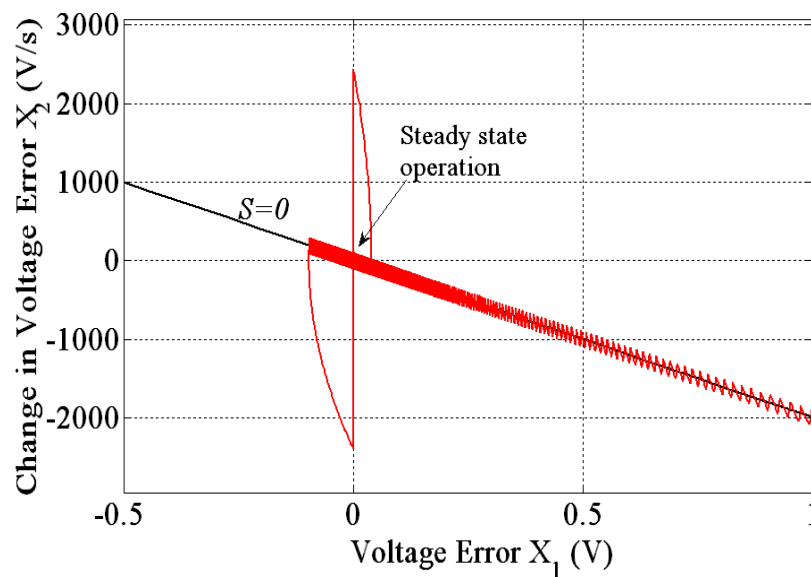


Figure 2.23: Phase plane plot under step load transient for SM control

2.7 Conclusion

The different control methods for dc-dc buck converter are discussed. The simulation results are also presented. The results of comparison are explained. The dynamic results in order to validate the disturbance rejection in larger range of variations are presented. The SM control method shows better dynamics for changes in input voltage and load compared to the PWM voltage-mode and current-mode control methods. It can be seen that the SM control method can well regulate the output voltage even in large range of load and line variation.

Chapter 3

CHAPTER 3

Fixed Frequency Hysteresis Control

3.1 Introduction

The use of hysteretic controllers for low voltage regulators used in computer and communication systems has been gaining interest due its various advantages. Advantages of this control approach includes fast response and robust with simple design and implementation. They do not require components for feedback loop compensation [6]-[8]. This reduces the number of components and size of theoretical analysis for implementation and also reduces the design effort for calculating the circuit component values (like inductor, capacitor, and input voltage). They response to disturbances and load change right after the transient takes place. Hence they give excellent transient performances. While the elimination of the compensation network allows for fast responses to transient, the hysteresis controlled converter suffers from two major drawbacks: variable switching frequency and non zero steady-state error. Non zero steady-state error may be rectified by adding a PI block in series with the voltage feedback. Also, the output voltage ripple is higher than the fixed band of hysteresis comparator. That is because of delays and output filter parasitic element. The application of nonlinear control theory can be used for study and analysis of hysteretic controlled converters for alleviating the above mentioned problems. This way of analysis gives a better idea for proper design method [6].

3.2 Variable Frequency Hysteretic Controllers

In this section, the basic ideas about the hysteretic controlled converters with variable switching frequency are described. As shown in Figure 3.1, the voltage hysteretic controller regulates the output voltage ripple within the hysteretic band. Similarly, a current hysteretic controller directly regulates the inductor current of the converter by regulating the inductor ripple or a scaled version of it within the hysteretic band.

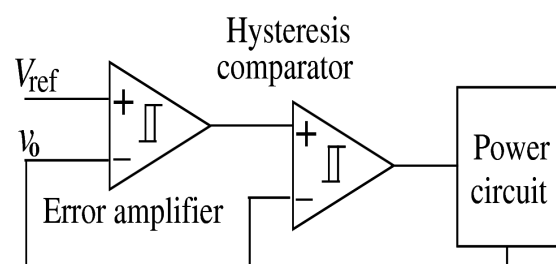


Figure 3.1: voltage hysteresis control

3.2.1 Hysteretic Voltage-Mode Controller

Hysteretic voltage-mode control is the simplest control method available. The concept of operation is very simple. The switch is turned on, when the output voltage falls below minimum set point (i.e., lower boundary) and turns off when output voltage is higher than maximum set point (i.e., upper boundary). Since the controller does not use a compensation network, the converter is able to react quickly to a transient event making it seem like a perfect solution for voltage regulator modules. However, the drawback of the voltage-mode hysteretic controller is its reliance on the converter's output capacitor parasitic. A block diagram of voltage hysteretic controlled converter is illustrated in Figure 3.1.

3.2.2 Hysteretic Current-Mode Controller

Hysteretic current-mode control functions by controlling both the peak inductor current and the valley inductor current. It does not require an external oscillator or saw-tooth generator for operation and it has the ability to provide a fast response to a transient event. Figure 3.2 illustrates a block diagram of a current-mode hysteretic controlled dc-dc converter.

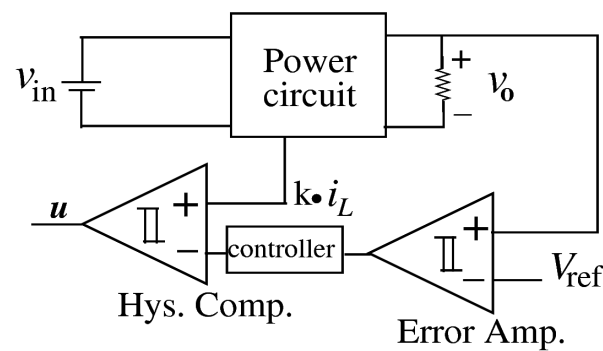


Figure 3.2: Hysteretic CM controlled buck converter

The power converter circuit with feedback control generally consists of:

1. a power stage with switches S_w and D , and storage elements L and C ,
2. an inner controller preserving the converter's working principle by switching the circuit topology,
3. an outer controller adjusting the inner loop's reference in response to deviations from the desired output.

The control system shown in figure 3.2 consists of two control loops. One is the current control loop and the other is the voltage control loop. The error between the actual output voltage and reference voltage gives the error voltage. A P or PI control block can use the voltage error signal to provide a reference current for hysteresis control. Hence the current hysteretic control method can be viewed as a sliding mode control system.

The hysteretic comparator implements the control law i.e.

$$u = \begin{cases} 1, & S > 0 \\ 0, & S < 0 \end{cases} \quad (3.1)$$

where, S is the sliding surface, which is defined as the difference between the two comparator inputs.

$$S = K_p (v_{ref} - v_0) - k \cdot i_L \quad (3.2)$$

where k is the current sensing gain which has a fixed value and K_p is proportional gain as we consider a proportional controller here. From the previous chapter, we know that the buck converter power circuit is described by two sets of differential equations that are,

$$L \frac{di_L}{dt} = v_{in} - v_0 \quad \text{and} \quad C \frac{dv_c}{dt} = i_L - \frac{v_0}{R} \quad (3.3)$$

Let the two state variable of the control system are $x_1 = V_{ref} - v_0$ and $x_2 = i_L$, then by taking the derivative,

$$\begin{aligned} L \dot{x}_2 &= v_{in} - v_{ref} + x_1 \\ \Rightarrow \dot{x}_2 &= \frac{1}{L} x_1 + \frac{v_{in}}{L} - \frac{v_{ref}}{L} \end{aligned} \quad (3.4)$$

and

$$\begin{aligned} x_2 &= C \dot{x}_1 + \frac{v_{ref} - x_1}{R} \\ \Rightarrow \dot{x}_1 &= -\frac{x_2}{C} - \frac{x_1}{RC} + \frac{v_{ref}}{RC} \end{aligned} \quad (3.5)$$

The state space model in terms of state variables is given by,

$$\dot{x} = A_1 x + B_1 u + D; \quad (3.6)$$

$$\begin{bmatrix} \dot{x}_1 \\ x_1 \\ \dot{x}_2 \\ x_2 \end{bmatrix} = \begin{bmatrix} -\frac{1}{RC} & \frac{1}{C} \\ \frac{1}{L} & 0 \end{bmatrix} \begin{bmatrix} x_1 \\ x_2 \end{bmatrix} + \begin{bmatrix} 0 \\ \frac{v_{in}}{L} \end{bmatrix} u + \begin{bmatrix} 0 \\ \frac{v_{ref}}{L} \end{bmatrix} \quad (3.7)$$

where ‘u’ is a discontinuous input that is either 0 or 1. The sliding dynamics of the system are obtained by using the equivalent control method [12]. The discrete form of the control input u is substituted with a continuous function u_{eq} . The dynamics of the closed loop system, assuming that an ideal sliding motion (infinite switching frequency) exists on the switching surface, ‘ S ’, is governed by the conditions,

$$\begin{aligned}
 S = 0 &\Rightarrow \dot{S} = 0 \\
 \Rightarrow \frac{ds}{dt} &= \sum_{i=1}^n \frac{\partial S}{\partial x_i} \frac{dx_i}{dt} \\
 \Rightarrow \frac{ds}{dt} &= \nabla S \cdot \dot{x} = G \dot{x}
 \end{aligned} \tag{3.8}$$

where G is a 1 by n matrix and the above equation is given as,

$$G \dot{x} = (A_1 x + B_1 u_{eq} + D_1) = 0$$

The equivalent continuous control input u_{eq} can be written as,

$$\begin{aligned}
 u_{eq} &= -(GB_1^{-1})G(A_1 x + D_1) \\
 \dot{x} &= A_1 x + D_1 - B_1 (GB_1^{-1})G(A_1 x + D_1) \\
 \Rightarrow \dot{x} &= [I - B_1 (GB_1^{-1})G](A_1 x + D_1)
 \end{aligned} \tag{3.9}$$

This equation describes motion equation of the converter when operating in SM operation.

3.3 Simulation Results

The simulation results are shown below derived for a current hysteresis controlled dc-dc buck converter with the same power circuit parameters that we have taken earlier in chapter 2. The effectiveness of hysteretic controlled converters is demonstrated through the results. Figure 3.3 shows the transient performance for step change in load from 15Ω to 10Ω and back to 15Ω. Figure 3.4 shows the transient response for input voltage variation from 20V to 15V and back to 20V.

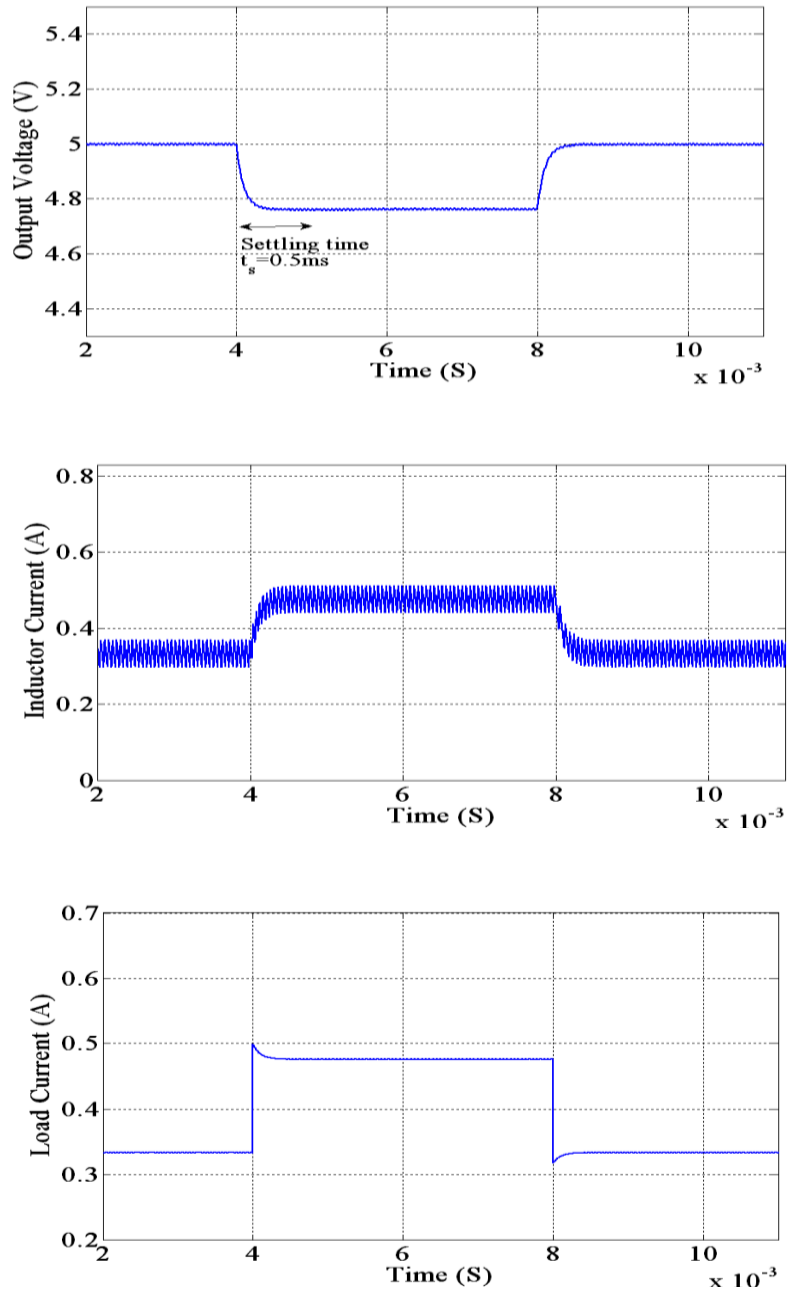


Figure 3.3: Transient response of the hysteretic current controlled buck converter when load changes from 15Ω to 10Ω and back 10Ω

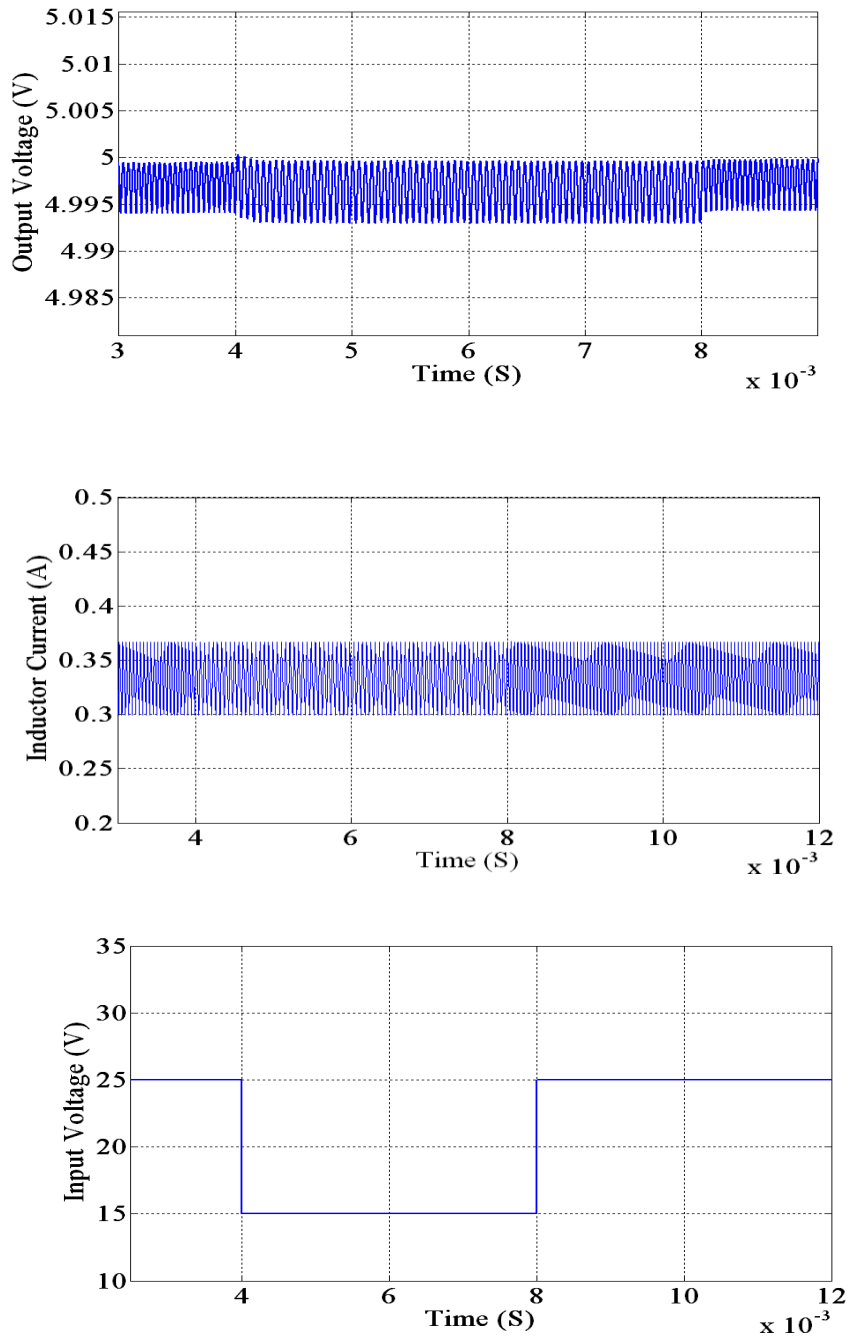


Figure 3.4: Transient response of the hysteretic current controlled buck converter when input voltage changes from 25V to 15V and back to 25V

From the results, it is seen that current hysteretic controller quickly responds to disturbances for large line and load variation. For a input voltage transient response, the current hysteretic controller has a negligible steady state error.

Phase plane analysis using the phase portrait is a very good graphical tool for analyzing the behavior of fast transient hysteretic control. This analysis is suitable for large signal analysis. By phase plane analysis method, the transient response is better understood and is shown in figure 3.5.

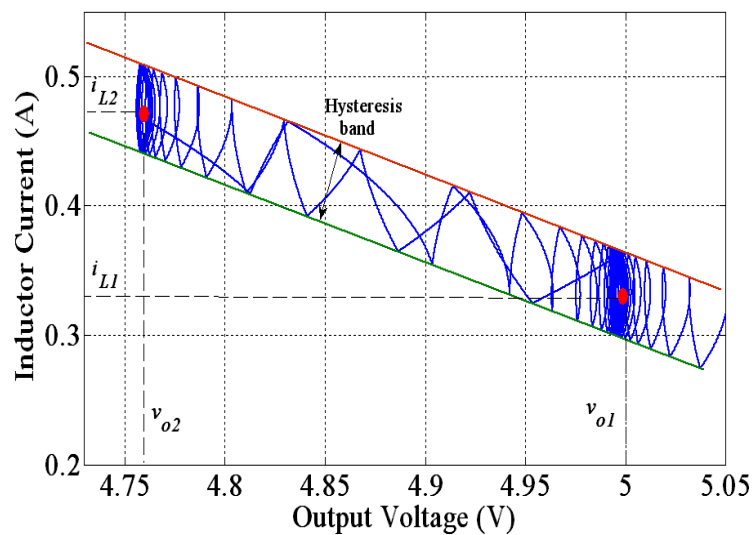


Figure 3.5: Phase portrait with load transient

In steady state the phase trajectory is on the stable equilibrium point. When transient occurs, the equilibrium is broken and the phase trajectory will direct towards a new equilibrium point and settles there again by making limit cycle.

3.4 Constant Switching Frequency Current-mode Hysteretic Controller

As discussed in previous chapter, different control techniques are used for controlling dc-dc converters. Some of the conventional control techniques are also described in previous chapter. In this section, a new control topology, which includes the concept of SM control and peak current mode control is proposed. Therefore the essential tools of the nonlinear control theory can be introduced for the study of this hysteresis controller. The proposed control scheme is actually a fixed frequency hysteretic current mode controller for dc-dc buck converter that operates in pseudo-CCM (PCCM) [64], [65]. In PCCM operation, the conventional buck converter circuit is modified by connecting an extra of switch across the inductor. This divides the total switching cycle into three subintervals which is termed as PCCM. The converter with this additional third interval is also known as tristate converter. Thus, the new control approach provides the advantages that are simple in implementation, fixed switching frequency operation, good transient performances and does not require a compensating ramp signal.

3.4.1 Basic Concept of Operation

The operation of the tristate dc-dc buck converter with hysteretic current-mode control scheme is discussed in this subsection. Figure 3.6 shows the tristate buck converter topology. It consists of two controlled switches S_1 and S_2 , an uncontrolled switch D , an inductor L and a capacitor C , a load resistance R . Switch S_2 is the additional switch which is connected across the inductor. The operation of the tristate converter includes three different configuration or structures that are show in figure 3.7.

At the start of the clock period, the switch S_1 is turned on and the switch S_2 is turned off.

During this interval (mode 1), inductor current increases with a slope of $\left(\frac{v_{in} - v_0}{L}\right)$.

When i_L reaches a peak value (upper bound), S_1 turns off. Then, i_L starts falling with a slope of $\left(\frac{-v_0}{L}\right)$ until it reaches some lower threshold. This interval is denoted as mode 2.

During this interval, diode is forward biased and both switch S_1 and S_2 are turned off.

When the inductor current reaches lower threshold, it stays constant at lower boundary,

because the switch S_2 shorts the inductor L and voltage across the voltage across the

inductor is thus equal to zero. During this interval S_2 is turned on while S_1 and diode are

off. This is the additional interval, denoted as mode 3. The inductor current waveform

showing the switch conditions for a tristate buck converter is shown in figure 3.8. All the

circuit components are assumed to be ideal in the derivations.

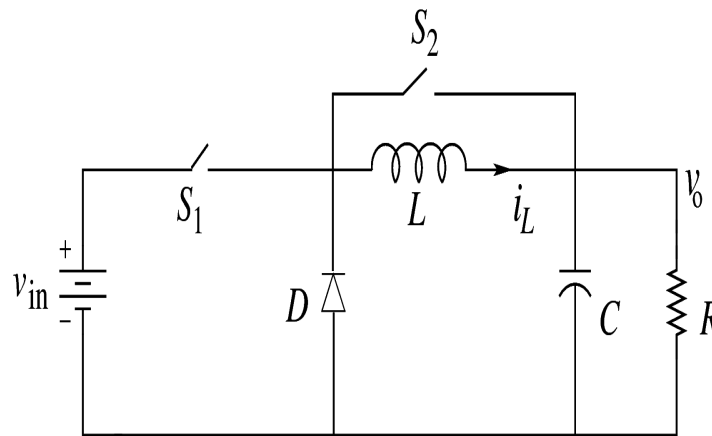
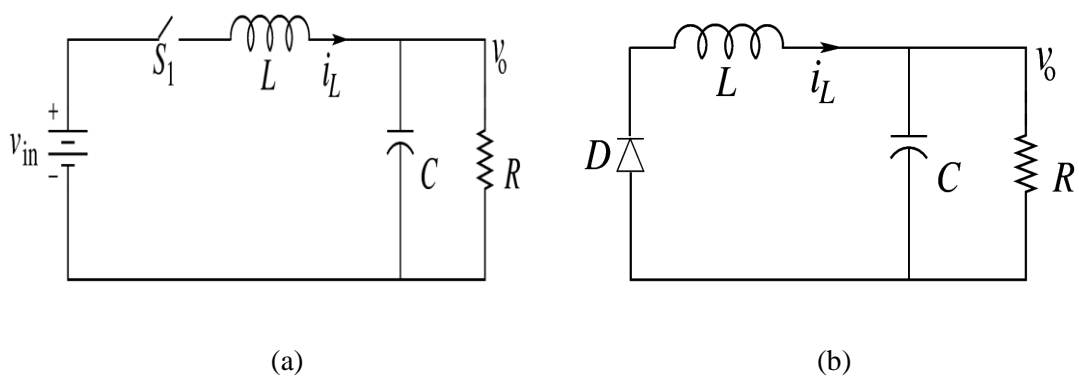
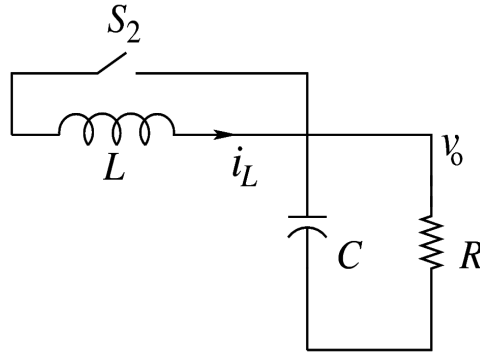


Figure 3.6: A tristate buck converter configuration





(c)

Figure 3.7: Equivalent circuits under different modes of operation: (a) mode 1 (D_1T_s), (b) mode 2 (D_2T_s), and (c) mode 3 (D_3T_s).

These three modes of operation can be described as follows:

Mode 1: when S_1 is on and, S_2 is off, the state space equation of buck converter is derived as

$$\frac{dx}{dt} = \begin{bmatrix} -\frac{1}{RC} & \frac{1}{C} \\ -\frac{1}{L} & 0 \end{bmatrix} x + \begin{bmatrix} 0 \\ \frac{1}{L} \end{bmatrix} v_{in} \quad (3.10)$$

where $x = [v_o \ i_L]^T$, v_o is the output voltage, i_L is the inductor current.

Mode 2: when S_1 and S_2 both are off, the equation is derived as,

$$\frac{dx}{dt} = \begin{bmatrix} -\frac{1}{RC} & \frac{1}{C} \\ -\frac{1}{L} & 0 \end{bmatrix} x + \begin{bmatrix} 0 \\ 0 \end{bmatrix} v_{in} \quad (3.11)$$

Mode 3: when S_1 is off, and S_2 is on, the state-space equation is

$$\frac{dx}{dt} = \begin{bmatrix} -\frac{1}{RC} & 0 \\ 0 & 0 \end{bmatrix} x + \begin{bmatrix} 0 \\ 0 \end{bmatrix} v_{in} \quad (3.12)$$

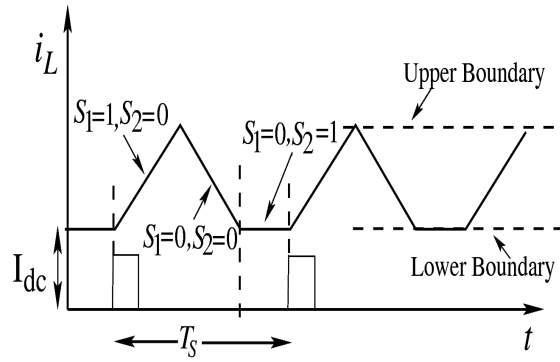


Figure 3.8: Inductor current waveform of tristate buck converter showing the switch conditions

3.4.2 Mathematical Analysis of Proposed Controller

The operation of a hysteretic current-mode controller for tristate dc-dc buck converter is proposed and the schematic diagram of proposed controller is shown figure 3.9.

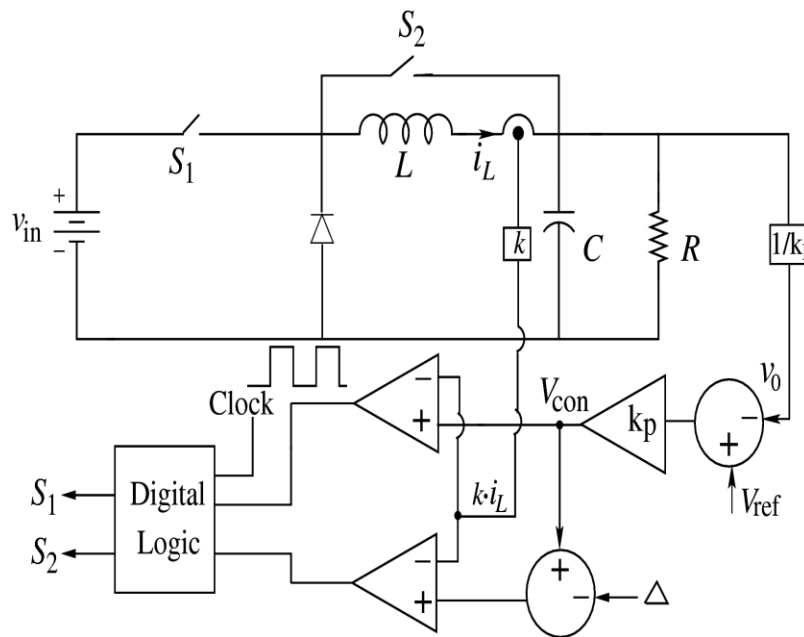


Figure 3.9: Schematic diagram of the hysteretic controller for tristate buck converter

The digital logic blocks generates required switching pulses for controlling the switches S_1 and S_2 . This block consists of two SR flip-flops and some logic gates that can be shown in figure 3.10.

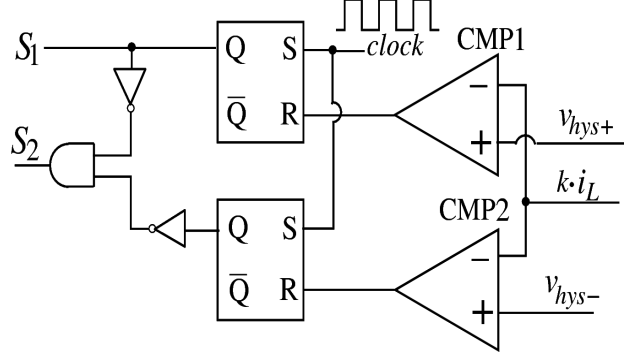


Figure 3.10: Schematic diagram of pulse generator circuit

The state-space description of the system in terms of the desired control variables (i.e., voltage, current etc) is developed. The proposed current controller employs both the output voltage error x_1 and the inductor current x_2 as the controlled state variables, which are expressed as

$$\begin{cases} x_1 = v_{ref} - v_0 \\ x_2 = i_L \end{cases} \quad (3.13)$$

where i_L represent the inductor current, v_0 and v_{ref} represent the output voltage and reference voltage respectively. Here the switching state of the switch is either 1 or 0.

Then by taking the derivative of (3.13) with respect to time,

$$\begin{aligned} \dot{x}_1 &= -\frac{dv_0}{dt} \\ \dot{x}_2 &= \frac{di_L}{dt} \end{aligned} \quad (3.14)$$

Considering the buck converter when the switch S_1 is on, S_2 off

$$L \frac{di_L}{dt} = v_{in} - v_0 \quad (3.15)$$

$$i_L = C \frac{dv_c}{dt} + \frac{v_0}{R} \quad (3.16)$$

Substituting equation (3.14) into equation (3.15) and (3.16) results in

$$\begin{aligned} \dot{x}_1 &= -\frac{1}{RC}x_1 - \frac{1}{C}x_2 + \frac{v_{ref}}{RC} \\ \dot{x}_2 &= \frac{1}{L}x_1 + \frac{v_{in}}{L} - \frac{v_{ref}}{L} \end{aligned} \quad (3.17)$$

The dynamics of the converter circuit, when S_1 and S_2 are off, can be expressed as,

$$L \frac{di_L}{dt} = -v_0 \quad (3.18)$$

$$i_L = C \frac{dv_c}{dt} + \frac{v_0}{R} \quad (3.19)$$

Substituting equation (3.14) into equation (3.18) and (3.19) results in

$$\begin{aligned} \dot{x}_1 &= -\frac{1}{RC}x_1 - \frac{1}{C}x_2 + \frac{v_{ref}}{RC} \\ \dot{x}_2 &= \frac{1}{L}x_1 - \frac{v_{ref}}{L} \end{aligned} \quad (3.20)$$

The dynamics of the converter circuit in mode 3, when S_2 is on, S_1 is off, can be expressed as,

$$L \frac{di_L}{dt} = 0 \quad (3.21)$$

$$i_L = C \frac{dv_c}{dt} + \frac{v_0}{R} \quad (3.22)$$

Since in this mode of operation, inductor current stays at a constant value, so we get the derivative of a constant value is zero. By substituting equation (3.14) into equation (3.21) and (3.22) results in,

$$\begin{aligned} \dot{x}_1 &= -\frac{1}{RC}x_1 \\ \dot{x}_2 &= 0 \end{aligned} \quad (3.23)$$

Then, the state-space modeling of the converter circuit with state variables x_1 and x_2 is given by,

$$\frac{dx}{dt} = \begin{cases} A_1x + B_1 + D_1; & \text{when } S_1 \text{ is on, and } S_2 \text{ is off} \\ A_2x + B_2 + D_2; & \text{when both } S_1 \text{ and } S_2 \text{ are off} \\ A_3x + B_3 + D_3; & \text{when } S_1 \text{ is off, and } S_2 \text{ is on} \end{cases} \quad (3.24)$$

where $x = [x_1 \ x_2]^T$ is the state vector and A's and B's are the system matrices.

The state matrices and the input vectors for the three periods are,

$$A_1 = A_2 = \begin{bmatrix} -\frac{1}{RC} & -\frac{1}{C} \\ \frac{1}{L} & 0 \end{bmatrix}, \quad A_3 = \begin{bmatrix} -\frac{1}{RC} & 0 \\ 0 & 0 \end{bmatrix},$$

$$B_1 = \begin{bmatrix} 0 \\ \frac{V_{in}}{L} \end{bmatrix}, \quad B_2 = \begin{bmatrix} 0 \\ 0 \end{bmatrix}, \quad D_1 = D_2 = \begin{bmatrix} \frac{1}{RC} \\ -\frac{1}{L} \end{bmatrix} V_{ref}, \quad D_3 = \begin{bmatrix} \frac{1}{RC} \\ 0 \end{bmatrix}$$

As studied from the previous discussion that the basic principles of a hysteresis control is based on the two hysteresis bands (upper and lower bands), whereby the controller turns the switch on when the output current falls below the lower band and turns the switch off when output is beyond the upper bound. The switching action can be determined in the following way,

1. If $i_L < \text{lower bound}$, $u = 1$ (ON)
2. If $i_L > \text{upper bound}$, $u = 0$ (OFF) , where u is the control input.

In this case, the hysteretic current controller shown in figure 3.2 consists of two control loops. One is the current control loop and the other is the voltage control loop. The difference between the actual output voltage and reference voltage generates the error voltage. A controller may a P or PI type use the voltage error signal to provide a control

voltage which is consider as the upper boundary or the upper threshold v_{hys+} . Here a simple proportional controller is considered for easy analysis. The control voltage v_{con} is a function of the output voltage v_0 and a reference signal V_{ref} in the form,

$$v_{con} = k_p (V_{ref} - v_0) \quad (3.25)$$

where, k_p is the gain of proportional controller. The lower threshold v_{hys-} , is determined by subtracting a small constant term Δ , which is given as, $v_{hys-} = v_{hys+} - \Delta$. Hence, there are two switching actions u_1 and u_2 are occurring on the two switching surfaces in the region of phase plane. The control law determines the switching action. This can be represented mathematically as,

$$u_1 = \begin{cases} 1, & \text{when } k \cdot i_L < v_{hys+} \text{ and } h_1 > 0 \\ 0, & \text{when } k \cdot i_L > v_{hys+} \text{ and } h_1 < 0 \end{cases} \quad (3.26)$$

$$u_2 = \begin{cases} 1, & \text{when } k \cdot i_L \leq v_{hys-} \text{ and } h_2 < 0 \\ 0, & \text{otherwise} \end{cases} \quad (3.27)$$

where h_1 and h_2 are the two switching surfaces (manifolds) in sliding mode phase plane that can be expressed as the combination of state variables,

$$\begin{aligned} h_1 &= k_p x_1 - k x_2 = c_1^T x \\ h_2 &= -k_p x_1 + k x_2 + \Delta = c_2^T x \end{aligned} \quad (3.28)$$

where x_1 and x_2 are the state variables, k is a constant factor that transforms the current signal to voltage signal, k_p is the proportional gain, which is known as sliding coefficient.

In the equations (3.26) and (3.27), u_1 and u_2 can be known as the discrete control inputs to the system and this equations forms the basis of control law for the hysteretic control system.

Generally a SM control design approach consists of two components. The first involves the design of a sliding surface and the second is concerned with the selection of a control law that directs the system trajectory towards system stable operating point. If we assume the width of the hysteresis band $\Delta \rightarrow 0$, then there exists only a single switching surface h_1 in phase plane. And for sliding mode to be exist on the switching surface, then $h_1 = 0$. This is said to be as ideal SM operation. Hence for ideal SM operation $dh_1/dt = \dot{h}_1 = 0$. Also the equivalent control produces trajectory whose motion is exactly equivalent to the trajectory's motion in an ideal SM operation [15]. In equivalent control, the discrete control input is substituted by continuous equivalent control signal u_{eq} and is obtained by solving the equations,

$$\begin{aligned}
dh_1/dt &= \dot{h}_1 = 0 \\
\Rightarrow c_1^T \dot{x} &= 0 \\
\Rightarrow c_1^T (A_1 x + B_1 u_{eq} + D_1) &= 0 \\
\Rightarrow u_{eq} &= -[c_1^T B_1]^{-1} c_1^T [A_1 x + D_1]
\end{aligned} \tag{3.29}$$

Then substituting the values, we get

$$\begin{aligned}
c_1^T A_1 x &= [k_p \ -k] \begin{bmatrix} -\frac{1}{RC} & -\frac{1}{C} \\ \frac{1}{L} & 0 \end{bmatrix} \begin{bmatrix} x_1 \\ x_2 \end{bmatrix} \\
\Rightarrow c_1^T A_1 x &= \left(-\frac{k_p}{RC} - \frac{k}{L} \right) x_1 - \frac{k_p}{C} x_2
\end{aligned} \tag{3.30}$$

$$\begin{aligned}
c_1^T B_1 &= [k_p \ -k] \begin{bmatrix} 0 \\ \frac{v_{in}}{L} \end{bmatrix} \\
\Rightarrow c_1^T B_1 &= -k \frac{v_{in}}{L}
\end{aligned} \tag{3.31}$$

$$c_1^T D_1 = [k_p - k] \begin{bmatrix} \frac{1}{RC} \\ -\frac{1}{L} \end{bmatrix} V_{ref} \quad (3.32)$$

$$\Rightarrow c_1^T D_1 = \frac{k_p V_{ref}}{RC} + \frac{k V_{ref}}{L}$$

$$c_1^T (A_1 x + B_1 u_{eq} + D_1) = 0 \quad (3.33)$$

$$\Rightarrow \left(-\frac{k_p}{RC} - \frac{k}{L} \right) x_1 - \frac{k_p}{C} x_2 - \frac{k v_{in}}{L} u_{eq} + \frac{k_p V_{ref}}{RC} + \frac{k V_{ref}}{L} = 0$$

From above equation (3.33), u_{eq} can be found as

$$u_{eq} = \frac{L}{k v_{in}} \left(-\frac{k_p}{RC} - \frac{k}{L} \right) V_{ref} - v_0 - \frac{k_p L}{C k v_{in}} i_L + \frac{k_p L V_{ref}}{R C k v_{in}} + \frac{V_{ref}}{v_{in}} \quad (3.34)$$

where u_{eq} is a smooth function of the discrete input function u and bounded by 0 and 1.

Then by substituting (3.21) into $0 < u_{eq} < 1$, the function can be expressed as,

$$0 < \frac{L}{k v_{in}} \left(-\frac{k_p}{RC} - \frac{k}{L} \right) v_{ref} - v_0 - \frac{k_p L}{C k v_{in}} i_L + \frac{k_p L V_{ref}}{R C k v_{in}} + \frac{V_{ref}}{v_{in}} < 1 \quad (3.35)$$

Multiplying the above equation by v_{in} ,

$$0 < \frac{L}{k} \left(-\frac{k_p}{RC} - \frac{1}{L} \right) v_{ref} - v_0 - \frac{k_p L}{C k} i_L + \frac{k_p L}{R C k} + V_{ref} < v_{in} \quad (3.36)$$

The SM existence region provides a range of sliding area where the sliding motion takes place. The condition for the existence of sliding mode is achieved, if the following inequalities are satisfied.

$$\begin{cases} \lim_{h_1 \rightarrow 0^+} h_1 \cdot \dot{h}_1 < 0 \\ \lim_{h_1 \rightarrow 0^-} h_1 \cdot \dot{h}_1 > 0 \end{cases} \quad (3.37)$$

$$\text{For } h_1 \rightarrow 0^+, \dot{h}_1 < 0: \dot{h}_1 = c_1^T (A_1 x + B_1 + D_1) < 0 \quad (3.38)$$

$$\text{For } h_1 \rightarrow 0^-, \dot{h}_1 < 0: \dot{h}_1 = c_1^T (A_1 x + B_1 + D_1) > 0 \quad (3.39)$$

By solving the above equations, we get,

$$L_1: \left(-\frac{k_p}{RC} - \frac{k}{L} \right) x_1 - \frac{k_p}{C} x_2 + \frac{k_p v_{ref}}{RC} + \frac{kv_{ref}}{L} - \frac{kv_{in}}{L} < 0 \quad \text{for } h_1 > 0 \quad (3.40)$$

$$L_2: \left(-\frac{k_p}{RC} - \frac{k}{L} \right) x_1 - \frac{k_p}{C} x_2 + \frac{k_p v_{ref}}{RC} + \frac{kv_{ref}}{L} > 0 \quad \text{for } h_1 < 0 \quad (3.41)$$

The above two equations represents two lines in phase plane with same slope. As there are two switching surfaces, so the SM existence region for hysteresis controlled converters can be found out by considering both the switching surfaces for analysis. From these equations we can find out the values of control parameters such that it will satisfy the existence condition.

3.5 Model including parasitic elements

The influence of parasitic elements on the converter behavior is not yet discussed. Therefore the circuit including the parasitic elements is given below. The tristate buck converter circuit consists of parasitic elements in the switches (r_1 and r_2), the capacitor (r_c), the inductor (r_L), and the diode (r_d), are shown in figure 3.11.

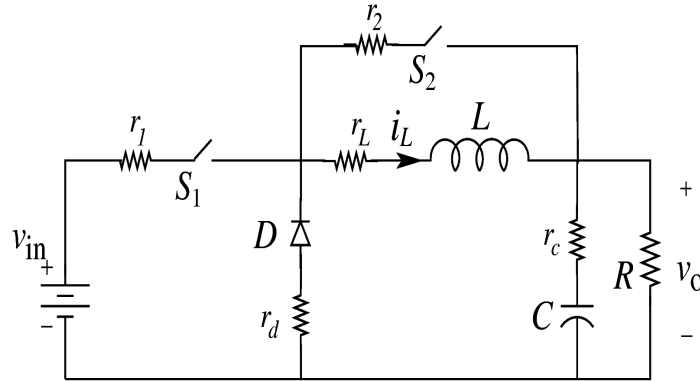


Figure 3.11: Model of tristate buck converter with all parasitic elements

The three modes of operation can be described as follows:

Mode 1: when S_1 is on and S_2 is off, the state space equation of buck converter is derived as

$$\frac{dx}{dt} = \begin{bmatrix} -\frac{1}{C(R+r_c)} & \frac{R}{C(R+r_c)} \\ -\frac{R}{L(R+r_c)} & -\frac{1}{L} \left((r_1+r_L) + \frac{Rr_c}{(R+r_c)} \right) \end{bmatrix} x + \begin{bmatrix} 0 \\ \frac{1}{L} \end{bmatrix} v_{in} \quad (3.42)$$

where $x = [v_c \ i_L]^T$, i_L is the inductor current, v_c is the output voltage.

Mode 2: when S_1 and, S_2 both are off, the equation is derived as,

$$\frac{dx}{dt} = \begin{bmatrix} -\frac{1}{C(R+r_c)} & \frac{R}{C(R+r_c)} \\ -\frac{R}{L(R+r_c)} & -\frac{1}{L} \left((r_d+r_L) + \frac{Rr_c}{(R+r_c)} \right) \end{bmatrix} x + \begin{bmatrix} 0 \\ 0 \end{bmatrix} v_{in} \quad (3.43)$$

Mode 3: when S_1 is off, and S_2 is on, the state-space equation is

$$\frac{dx}{dt} = \begin{bmatrix} -\frac{1}{C(R+r_c)} & 0 \\ 0 & -\frac{r_L+r_2}{L} \end{bmatrix} x + \begin{bmatrix} 0 \\ 0 \end{bmatrix} v_{in} \quad (3.44)$$

3.6 Simulation Results

In this subsection, based on the above proposed hysteretic current control method, the simulation studies have been performed on a dc-dc buck converter under steady-state and also under dynamic conditions of line and load variations. The buck converter parameters chosen for the simulation studies are input voltage $v_{in}=20V$, desired output voltage $v_0=5V$, inductance $L=3mH$, capacitance $C=69\mu F$, minimum load resistance $R_{min}=10\Omega$, maximum load resistance $R_{max}=15\Omega$, voltage reduction factor $k_1=0.8$, proportional gain

$k_p=2$, delta $\Delta=0.03$, and current sensing gain $k=3\Omega$. The switching frequency f_s is set to 100 kHz. A simple proportional controller is considered here. The simulations are done using MATLAB/SIMULINK.

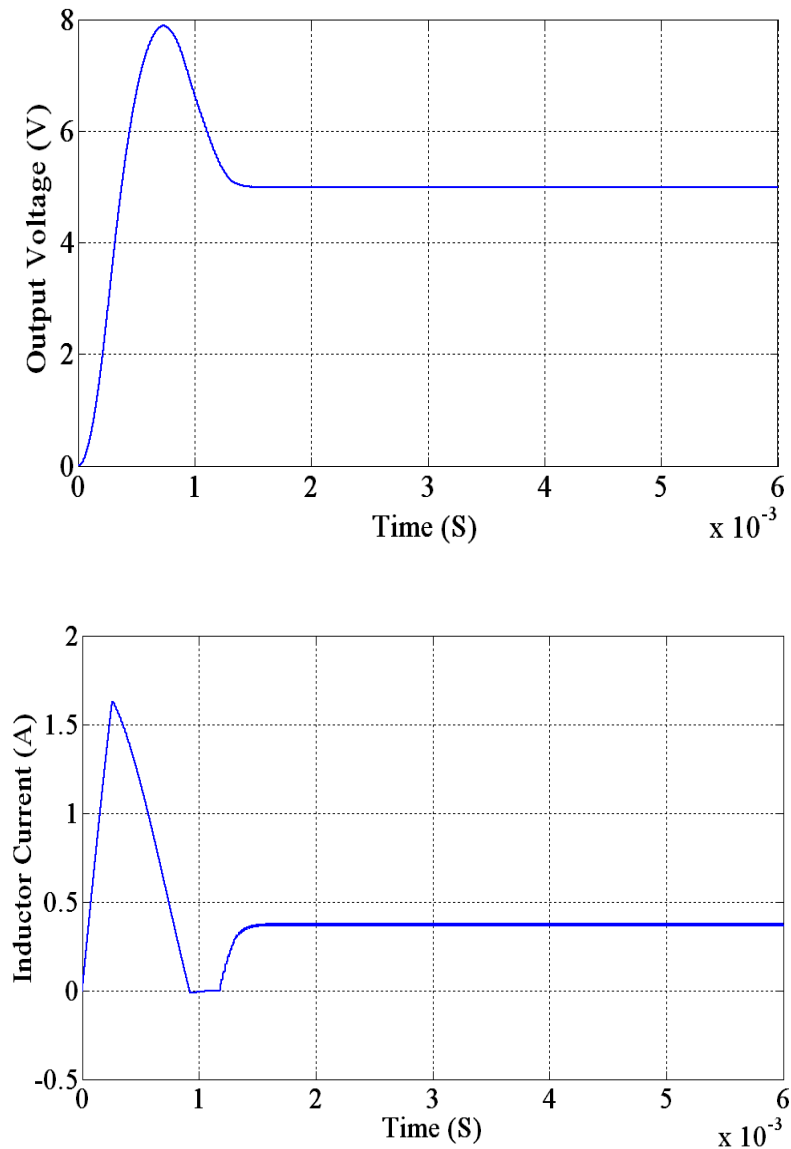


Figure 3.12: Start-up transient performance of the converter with the proposed controller

The current hysteric control converter operated in PCCM operation showed less current and voltage ripple. From the results, we got the value of output voltage ripple and inductor current ripple as 0.005 V and 0.012A in steady state.

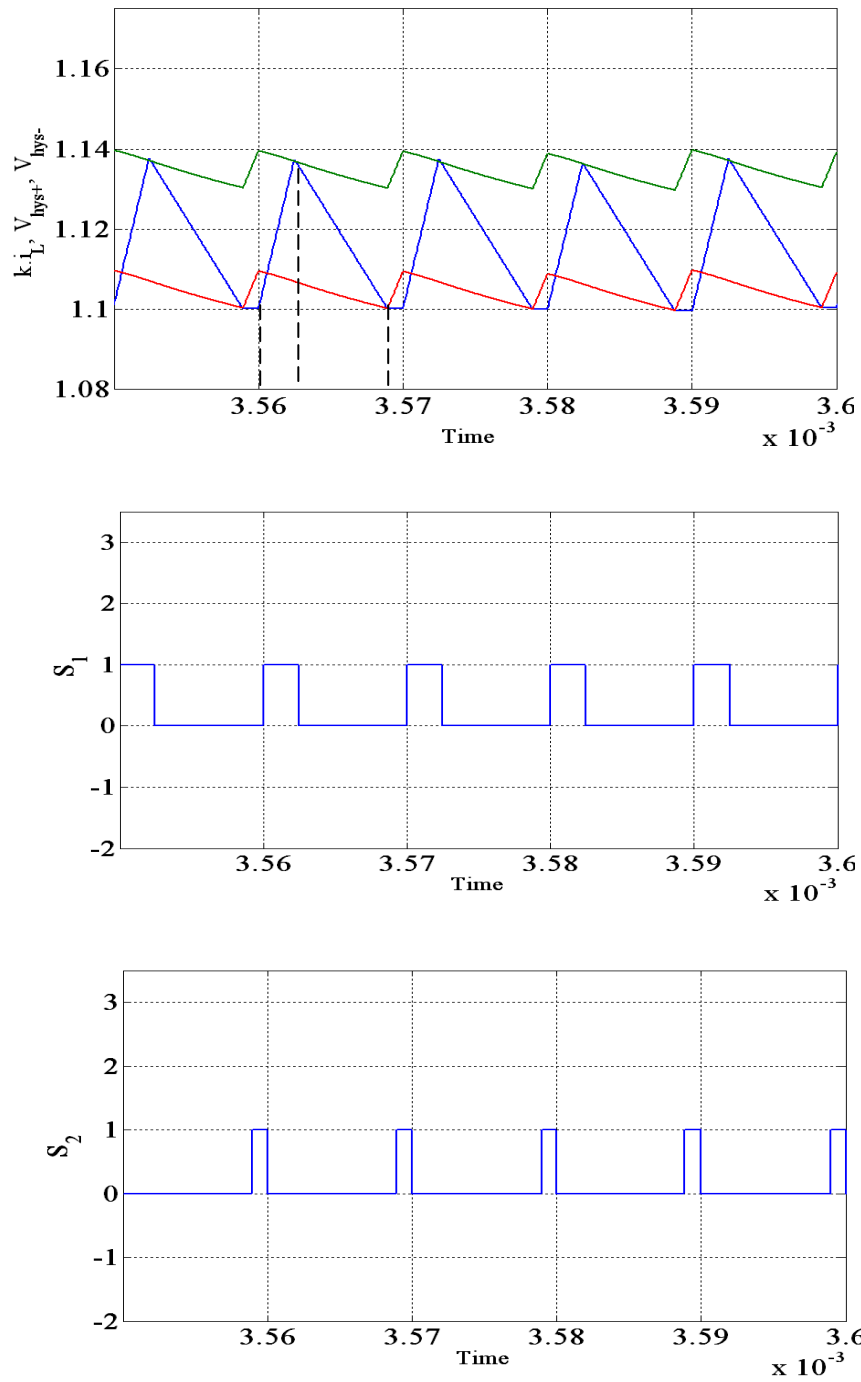


Figure 3.13: The proposed current hysteretic controller operating principle

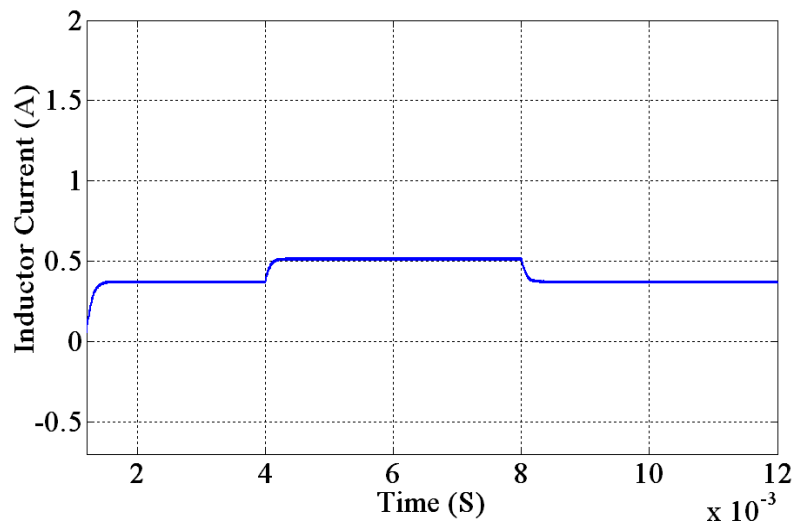
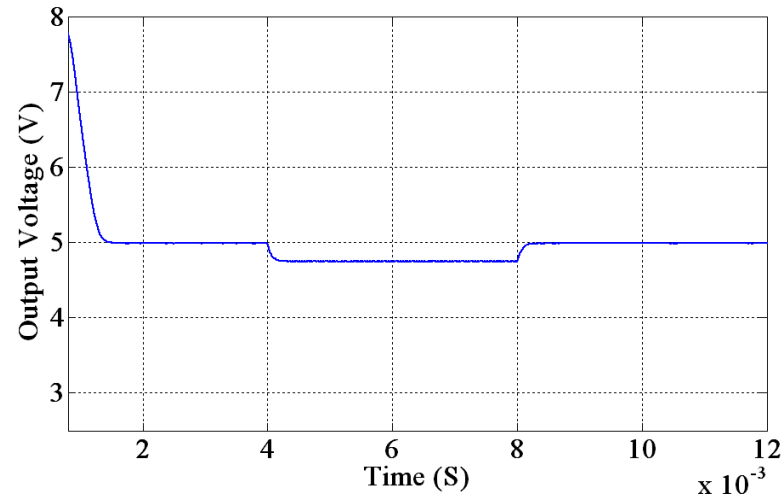


Figure 3.14: Transient response for change in load from 15Ω to 10Ω and back to 15Ω

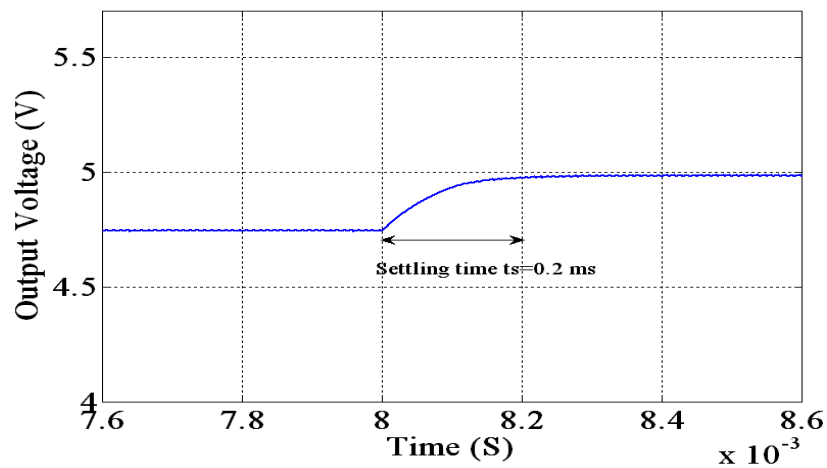


Figure 3.15: Output voltage response from load transient 10Ω to 15Ω

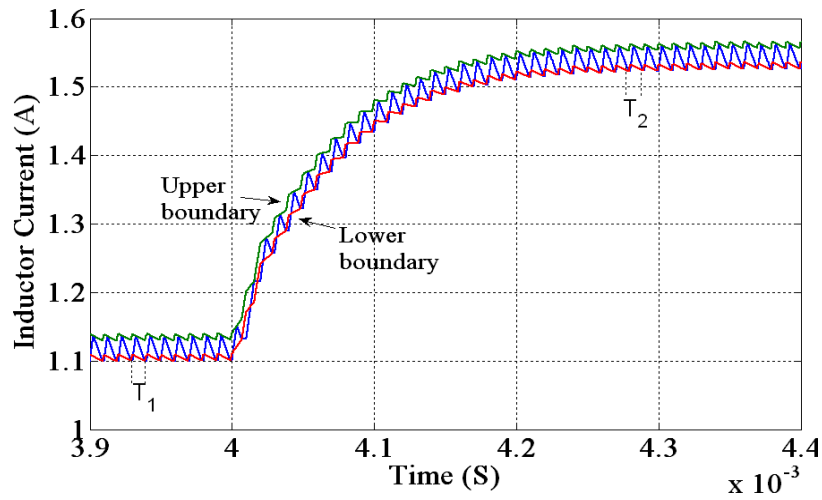


Figure 3.16: Load transient response from 15Ω to 10Ω

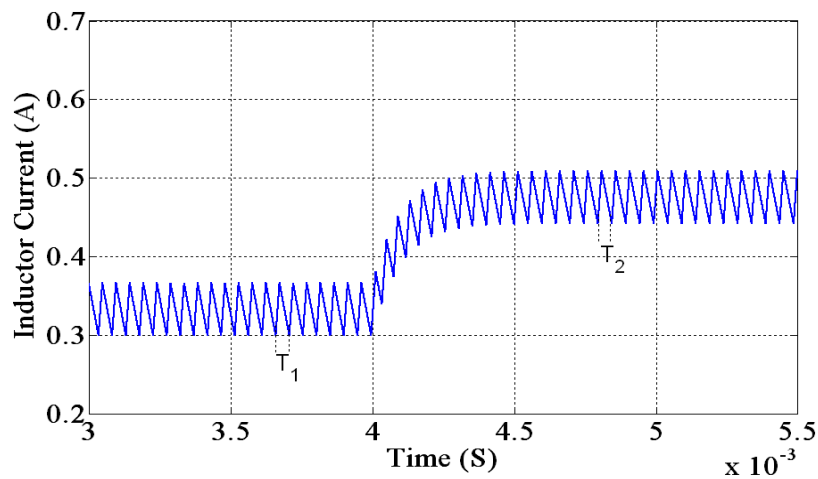


Figure 3.17: Load transient response from 15Ω to 10Ω for conventional current hysteric control method

From figure 3.16 and 3.17, it is seen that in case conventional current hysteric control method the switching frequency is not constant ($T_1 \neq T_2$) when load is varied. But for the proposed control technique we are getting a fixed switching frequency ($T_1 = T_2$) when load varies.

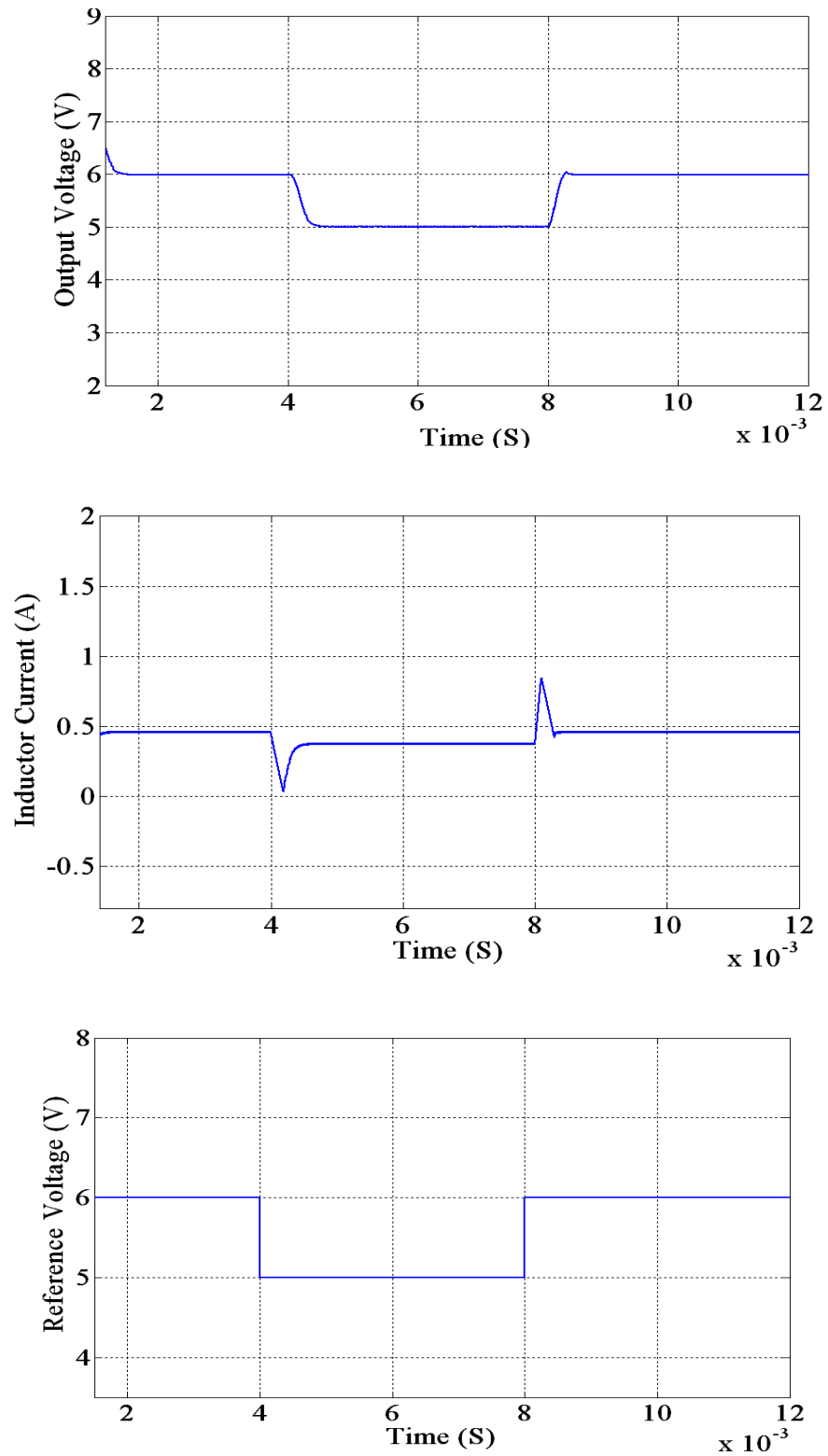


Figure 3.18: Transient response due to a step change in reference voltage from 6V to5V and back to 6 V

Figure 3.19 shows the motion of the phase trajectory in two dimensional plane. In this case three states exist on phase plane. When the phase trajectory hits the lower boundary, system status changes to first sub circuit state. When it touches the upper boundary, system status changes to second sub circuit state and again when it touches the lower boundary, system status changes to third sub circuit state for a fixed period. With these switching actions, the trajectory slide within the hysteretic band towards the system steady state operating point and makes a limit cycle around that point. Hence, the states are regulated in one operating point by means of control law.

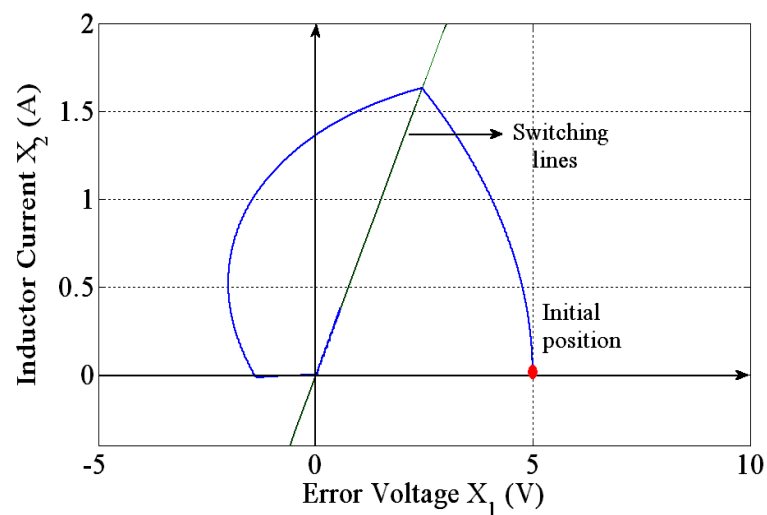


Figure 3.19: phase plane diagram

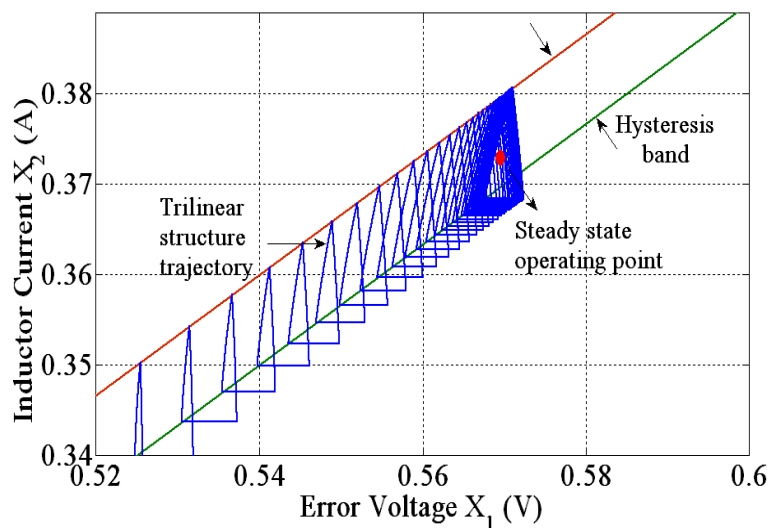


Figure 3.20: Magnified view showing the phase trajectory and hysteresis band

The simulation results for the buck converter with the proposed current hysteretic controller including all the parasitic elements are shown in following figures. The values of the resistive parasitic components are chosen as: $r_1 = 2.1 \text{ m}\Omega$, $r_2 = 0.2 \text{ }\Omega$, $r_c = 5.5 \text{ m}\Omega$, $r_L = 0.8 \text{ }\Omega$, $r_d = 2.1 \text{ m}\Omega$ respectively.

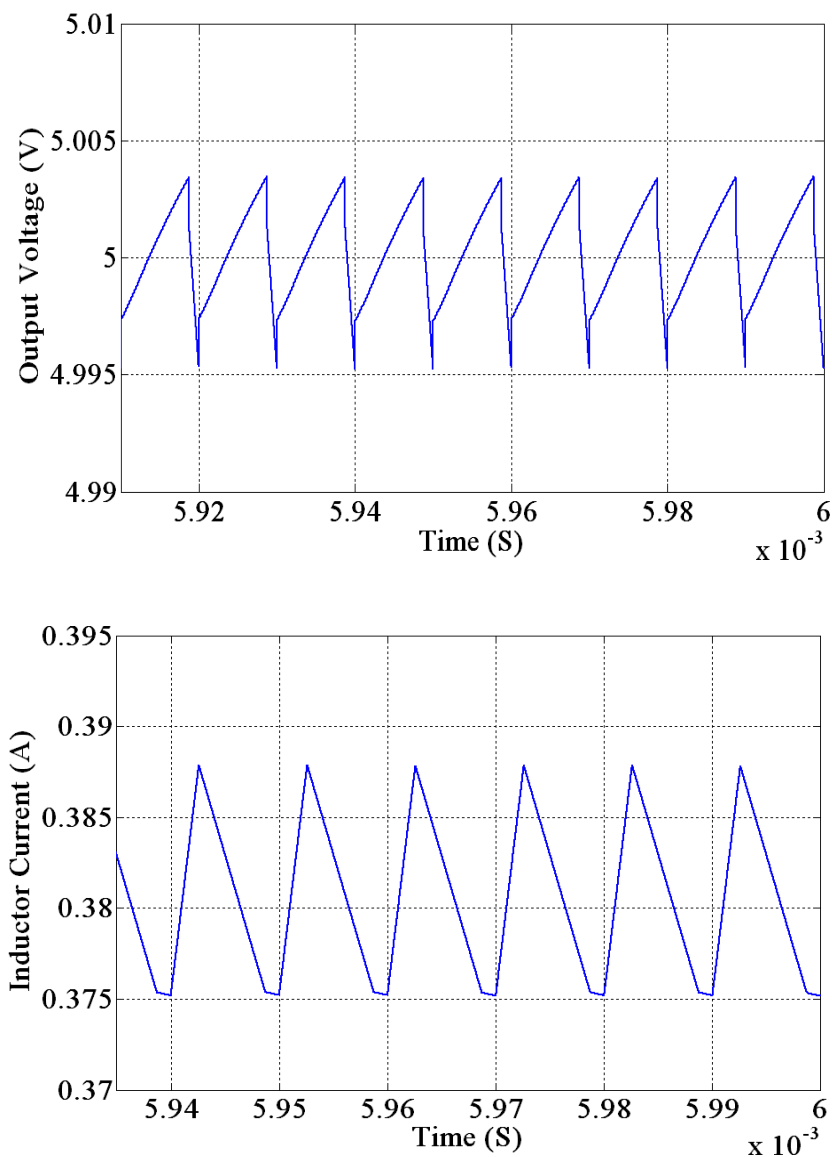


Figure 3.21: The output voltage ripple and inductor current ripple in steady state operation by considering the effect of parasitic elements

To increase the duration of mode 3 the level of lower boundary must be increased. Therefore to increase the level of lower lower boundary that is $v_{hys-} = v_{hys+} - \Delta$, the value of Δ is decreased. So Δ value is taken as 0.02. The inductor current ripple in steady state operation is shown in figure 3.22 that shows the longer duration for mode 3.

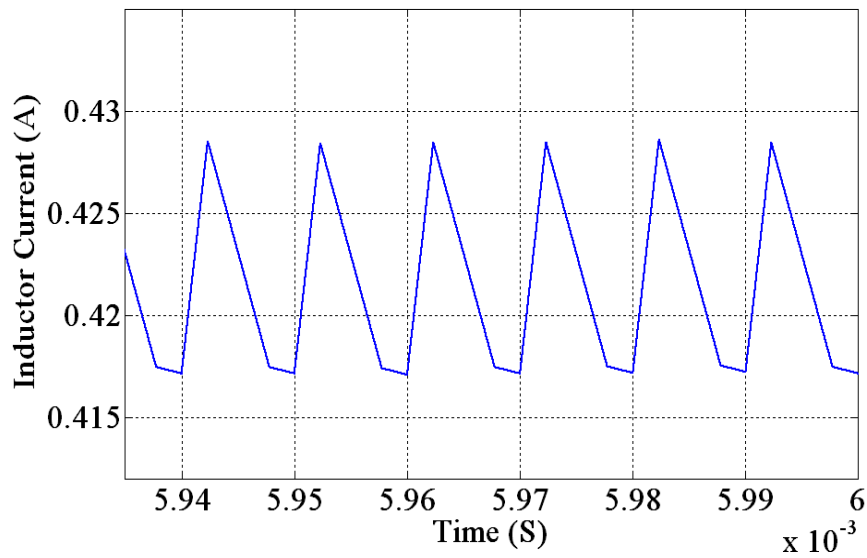


Figure 3.22: The inductor current ripple in steady state operation

3.7 Conclusion

In this chapter, the principle and operation of different types of hysteresis controllers are discussed. The effectiveness of hysteretic controller for faster transient response is described through the simulation results. The main problem associated with these conventional hysteretic controlled converters is variable switching frequency operation. Thus a constant switching frequency hysteretic controller is proposed. The controller is of current-mode operation. The proposed controller is simple in design and implementation without the use of compensating ramp circuit. The steady state and transient responses are presented. The result shows good performances.

Chapter 4

CHAPTER 4

Conclusions

4.1 Conclusions

This chapter summarizes the contributions and the main results of the thesis. The thesis has explained about the merits and demerits of different control methods such as the PWM voltage mode control, peak current mode control, hysteresis control and sliding mode control for dc-dc buck converter. A fixed frequency current hysteresis control has been designed for buck converter.

Chapter 1 describes the importance and application of switch mode dc-dc converter. The various control schemes used for dc-dc converters has been explained in brief. A review study on the previous work in this area has been presented. The main frame of the work and also the work done in each chapter has been described.

In **chapter 2** a detailed explanation and classification of existing control techniques for switched mode power supplies have been given. The chapter also defined and summarized, with the aid of mathematical equations for dc-dc buck converter. The information about the different modes of operations that are continuous conduction mode (CCM), discontinuous conduction mode (DCM) has been given. A comparison study has been carried out for studying the effects of PWM controllers and SM control on the dc-dc buck converter response in steady state, under line variations, load variations, and different component variations.

Chapter 3 gives a detail study on hysteretic control dc-dc converters. The advantages and drawbacks of main types of hysteretic controllers i.e. voltage hysteresis control and current hysteresis control has been explained. The principle of operation of tristate buck converter was given. A hysteretic current control technique for a tri-state buck converter operating in constant switching frequency has been designed and behavior of the controller is studied by using sliding mode control theory because dc-dc buck converter is a variable structure system due to the presence of switching actions. The converter response has been investigated in the steady-state region and in the dynamic region.

The main work of this thesis can be summarized as follows:

- Study of the PWM voltage mode control, PWM current mode control and their operation has been given. The advantages and drawbacks of each control method when implemented in switched-mode power converters are shown.
- The analysis and the theories of SM control were given in details. SM control implemented in dc-dc buck converter is presented. Then a comparative analysis on conventional PWM controllers and SM control has been done. The simulated result showed the satisfying theories of SM control. The advantages of SM control over other control methods are described.
- The basic concept of operation of tristate buck converter has been studied. The implementation of fixed frequency hysteretic current control to the tristate buck converter has been given. The output voltage, main inductor current waveforms were studied in steady-state region and in dynamic region.

4.2 Scope of Future Work

Following are the areas of future study which can be considered for further research work.

- The proposed control method is applied on dc-dc buck converter. It can be applied to many other converter topologies. The non zero steady state error is minimized by adding PI block in the feedback control loop.
- The using the sliding mode control concept used for studying the behavior of hysteretic controlled dc-dc buck converter can be extended for other converter topologies.
- To verify the theoretical study, the proposed control scheme can be done with experimental prototype.

References

References

- [1] M. H. Rashid, *Power Electronics: Circuits, Devices and Applications (3rd Edition)*, Prentice Hall, 2003.
- [2] N. Mohan , T. M. Undeland, W. P. Robbins, *Power Electronics: Converters, Applications, and Design, 3rd Bk&Cdr edition*, Wiley, 2002.
- [3] R.D Middlebrook and S Cuk , “A general unified approach to modeling switching Converter Power stages,” in *Proc. IEEE PESC Rec.*, pp. 18–34, 1976.
- [4] A.J. Forsyth and S.V. Mollow, “Modeling and control of dc-dc converters,” *IEE power engineering journal*, vol. 12, no. 5, pp. 229–236, Oct. 1998.
- [5] V.S.C Raviraj and P.C. Sen, “Comparative Study of proportional-integral, Sliding-mode, and fuzzy logic controllers for power converters,” *IEEE transaction on Industry applications*, vol. 33, no. 2, pp. 518-524, Mar. /Apr. 1997.
- [6] M. Castilla, L. G. de Vicuna, J.M. Guerrero, J. Matas, and J. Miret, ‘Design of voltage-mode hysteretic controllers for synchronous buck converters supplying microprocessor loads’, *IEE Proceedings on Electrical Power Applications*, Vol.152, No. 5, pp.1171–1178, Sep. 2005.
- [7] M. Castilla, L. G. de Vicuna, J.M. Guerrero, J. Miret, and N. Berbel, ‘Simple low-cost hysteretic controller for single-phase synchronous buck converter’, *IEEE Transactions on Power Electronics*, Vol. 22, No. 4, pp.1232–1241, Jul. 2007.
- [8] M. Castilla, L. G. de Vicuna, J.M. Guerrero, J. Matas, and J. Miret, ‘Designing VRM hysteretic controllers for optimal transient response’, *IEEE Transactions on Industrial Electronics*, Vol. 54, No. 3, pp.1726–1738, Jun. 2007.

- [9] T. Nabeshima, T. Sato, S. Yoshida, S. Chiba, and K. Onda, "Analysis and design considerations of a buck converter with a hysteretic PWM controller," in *Proc. IEEE PESC*, pp. 1711–1716, 2004.
- [10] V. Utkin, J. Guldner, and J. X. Shi, *Sliding Mode Control in Electromechanical Systems*. London, U.K.: Taylor & Francis, 1999.
- [11] C. Edwards and S. K. Spurgeron, *Sliding Mode Control: Theory and Applications*. London, U.K.: Taylor & Francis, 1998.
- [12] R. Venkataramanan, "Sliding mode control of power converters," *Ph.D. dissertation, California Inst. Technol., Dept. Elect. Eng., Pasadena, CA*, May 1986.
- [13] F. Bilalovic, O. Music and A. Sabanovic, "Buck converter regulator operating in sliding mode," in *Proc. 7th Int. Conf.PCI*, pp. 331-340, Apr. 1983.
- [14] R. Venkataramanan, A. Sabanovic, and S. Cuk, "Sliding mode control of DC-to-DC converters," in *Proc. IEEE Conf. IECON*, pp. 251-258, 1985.
- [15] S. C. Tan, Y. M. Lai, C. K. Tse, "General design issues of sliding-mode controllers in dc-dc converters," *IEEE Trans. Industrial Electronics.*, vol. 55, no. 3, pp. 1160–1174, Mar. 2008.
- [16] S.P Huang, H.Q. Xu, and Y.F. Liu. L, "Sliding mode controlled Cuk switching regulator with fast response and first-order dynamic characteristics," in *Proc. IEEE PESC Rec.*, pp. 124-129, Jun. 1989.
- [17] E. Fossas, L. Martinez, and j. Ordinas, "Sliding-mode control reduces audio susceptibility and load perturbation in the Cuk converter," *IEEE Trans. Circuits Syst. I. Fundam. Theory Appl.*, vol. 39, no. 10, pp. 847-849, Oct. 1992.
- [18] L. Malesani, L. Rossetto, G. Spiazzi, and P. Tenti, "Performance optimization of Cuk converters by sliding-mode control," *IEEE Trans. Power Electron.*, vol. 10, no. 3, pp. 302-309, May 1995.

- [19] M. Oppenheimer, M. Husain, M. Elbuluk, and J. A. De Abreu Garcia, "Sliding mode control of cuk converter," in *Proc. IEEE PESC Rec.*, vol. 2, pp. 1519-1526, Jun. 1996.
- [20] J. Mahadavi and A. Emadi, "Sliding-mode control of PWM Cuk converter," in *Proc. 6th Int. Conf. Power Electron. Variable Speed Drives*, vol. 2, pp. 372-377, Sep. 1996.
- [21] E. Fossas and A. Pas, "Second order sliding mode control of a buck converter," in *Proc. 41st IEEE Conf. Decision Control*, vol. 1, pp. 346-347, Dec. 2002.
- [22] Y. B. Shtessel, A. S. I. Zinober, and I. A. Shkolnikov, "Boost and buck-boost power converters control via sliding modes using method of stable system centre," in *Proc. 41st IEEE Conf. Decision Control*, vol. 1, pp. 346-347, Dec. 2002.
- [23] Y. B. Shtessel, A. S. I. Zinober, and I. A. Shkolnikov, "Boost and buck-boost power converters control via sliding modes using dynamic sliding manifold," in *Proc. 41st IEEE Conf. Decision Control*, vol. 3, pp. 2456-2461, Dec. 2002.
- [24] H. Sira-Ramirez, "Sliding mode- Δ modulation control of a "buck converter"," in *proc. 42nd IEEE Conf. Decision control*, vol. 3, pp. 2999-3004, Dec. 2003.
- [25] H. Sira-Ramirez, "On the generalized PI sliding mode control of DC-TO-DC power converters: A tutorial," *Int.J. Control*, vol. 76, no. 9/10, pp. 1018-1033, 2003.
- [26] V. S. C. Raviraj and P. C. Sen, "Comparative study of proportional integral, sliding mode, and fuzzy logic controllers for power converters," *IEEE Trans. Ind. Appl.*, vol. 33, no. 2, pp. 518-524, Mar./Apr. 1997.
- [27] P. F. Donoso-Garcia, P. C. Cortizo, B. R. de Menez, and M. A. Severo Mendes, "Sliding mode control for current distribution in DC-to-DC converters connected in parallel," in *proc. IEEE PESC Rec.*, pp. 1513-1518, Jun. 1996.
- [28] Y. B. Shtessel, O. A. Raznopolov, and L. A. Ozerov, "Sliding mode control of multiple modular DC-to-DC power converters," in *Proc. IEEE Int. Conf. Control Appl.*, pp. 685-690, Dec. 1996.

- [29] H. Sira-Ramirez and M. Rios-Bolivar, "Sliding mode control of DC-to-DC power converters via extended linearization," *IEEE Trans. Circuit Syst. I, Fundum Theory Appl.*, vol. 41, no. 1, pp. 652-651, Oct. 1994.
- [30] H. Sira-Ramirez, R. Ortega, R. Perez-Moreno, and M. Garcia-Esteban, "A sliding mode controller-observer for DC-to-DC power converters: A passivity approach," in *Proc. 34th IEEE Conf. Decision Control*, pp. 3379-3784, Dec.1995.
- [31] H. Sira-Ramirez, G. Escobar, and R. Ortega, "On passivity-based sliding mode control of switched DC-to-DC power converters," in *Proc. 35th IEEE Conf. Decision Control*, pp. 2525-2526, Dec.1996.
- [32] J. M. Carrasco, J. M. Quero, F. P. Ridaio, M. A. Perales and L. G. Fanquelo, "Sliding mode control of a DC/DC PWM converter with PFC implemented by neural networks," *IEEE Trans. Circuits Syst. I, Fundam, Theory Appl.*, vol. 44, no. 8, pp. 743-749, Aug. 1997.
- [33] C. Morel, "Application of slide mode control to a current mode control boost converters," in *Proc .IEEE Conf. IECON*, vol. 3, pp. 1824-1829, Nov. 2002.
- [34] C.Morel,J.C. Guignard, and M.Guillet, "Sliding mode control of DC-to-DC power converters,"in *Proc. 9th Int. Conf. Electron., Circuits Syst.*, vol. 3,pp.971-974, Sep.2002.
- [35] C. Morel, "Slide mode control via current mode control in DC-DC converters," in *Proc .IEEE Int. Conf. Syst., Man. Cybern.*, vol. 5, pp. 6-11, Oct. 2002.
- [36] P. Mattavelli, L. Rossetto, G. Spiazzi, and P. Tenti, "General-purpose sliding-mode controller for DC/DC converter applications," in *Proc. IEEE PESC Rec.*, pp. 609–615, Jun. 1993.
- [37] P. Mattavelli, L. Rossetto, and G. Spiazzi, "Small-signal analysis of DC–DC converters with sliding mode control," *IEEE Trans. Power Electron.*, vol. 12, no. 1, pp. 96–102, Jan. 1997.

- [38] G. Escobar, R. Ortega, H. Sira-Ramirez, J. P. Vilain, and I. Zein, “ An experimental comparison of several nonlinear controllers for power converters,” *IEEE Control Syst. Mag.*, vol. 19, no. 1, pp. 66-82, Feb. 1999.
- [39] E. Alarcon , A. Romero, A. Poveda, S. Porta and L. Martinez-Salamero, “Sliding-mode control analog integrated circuit for switching DC-DC power converter,” in *Proc. IEEE Int. Symp. Circuits Syst.*, pp. 500-503, May 2001.
- [40] M. Ahmed, M. Kuisma, K. Tosla, and P. Silventoinen, “Implementing sliding mode control for buck converter,” in *Proc. IEEE PESC Rec.* , vol. 2, pp. 634-637, Jun. 2003.
- [41] M. Ahmed, M. Kuisma, K. Tosla, P. Silventoinen, and O. Pyrhonen, “Effect of implementing sliding mode control on the dynamic behavior and robustness of switch mode power supply(buck converter),” in *Proc. 5th Int. Conf. Power Electron. Drive Syst.*, vol. 2, pp. 1364-1368, Nov. 2003.
- [42] M. Ahmed, M. Kuisma, O. Pyrhonen and, P. Silventoinen, “Sliding mode control of buck boost converter using control desk dSPACE,” in *Proc. 5th Int. Conf. Power Electron. Drive Syst.*, vol. 2, pp. 1491-1494, Nov. 2003.
- [43] F. Dominguez, E. Fossas, and L. Martinez, “Stability analysis of a buck converter with input filter via sliding-mode approach,” in *Proc. IEEE Conf. IECON*, pp. 1438–1442, Sep. 1994.
- [44] ZHANG Li, QIU Shui-sheng, “Analysis and Experimental study of Proportional-Integral sliding mode control for dc/dc converter,” *Journal of Electronic Science and Technology of China*, vol. 3, no. 2, pp. 140-143, Jun. 2005.
- [45] M. Castilla, L. C. de Vicuna, M. Lopez, O. Lopez, and J. Matas, “On the design of sliding mode control schemes for quantum resonant converters,” *IEEE Trans. Power Electron.*, vol. 15, no. 6, pp. 960–973, Nov. 2000.

- [46] S. C. Tan, Y. M. Lai, M. K. H. Cheung, and C. K. Tse, "On the practical design of a sliding mode voltage controlled buck converter," *IEEE Trans. Power Electron.*, vol. 20, no. 2, pp. 425–437, Mar. 2005.
- [47] S. C. Tan, Y. M. Lai, C. K. Tse, and M. K. H. Cheung, "A fixed-frequency pulse-width-modulation based quasi-sliding mode controller for buck converters," *IEEE Trans. Power Electron.*, vol. 20, no. 6, pp. 1379–1392, Nov. 2005.
- [48] B. J. Cardoso, A. F. Moreira, B. R. Menezes, and P. C. Cortizo, "Analysis of switching frequency reduction methods applied to sliding mode controlled DC–DC converters," in *Proc. IEEE APEC*, pp. 403–410, Feb. 1992.
- [49] S. C. Tan, Y. M. Lai, C. K. Tse, and M. K. H. Cheung, "A pulse-width modulation based sliding mode controller for buck converters," in *Proc. IEEE PESC'04*, pp. 3647–3653, Jun. 2004.
- [50] V. M. Nguyen and C. Q. Lee, "Tracking control of buck converter using sliding-mode with adaptive hysteresis," in *Proc. IEEE PESC Rec.*, vol. 2, pp. 1086–1093, Jun. 1995.
- [51] V. M. Nguyen and C. Q. Lee, "Indirect implementations of sliding-mode control law in buck-type converters," in *Proc. IEEE APEC*, vol. 1, pp. 111–115, Mar. 1996.
- [52] H. Chiacchiarini, P. Mandolesi, and A. Oliva, "Nonlinear analog controller for a buck converter: Theory and experimental results," in *Proc. IEEE Int. Symp. Ind. Electron.*, pp. 601–606, Jul. 1999.
- [53] H. Sira-Ramirez and M. Ilic, "A geometric approach to the feedback control of switch mode DC-to-DC power supplies," *IEEE Trans. Circuits Syst.*, vol. 35, no. 10, pp. 1291–1298, Oct. 1988.
- [54] H. Sira-Ramirez, "A geometric approach to pulsewidth modulated control in nonlinear dynamical systems," *IEEE Trans. Autom. Contr.*, vol. 34, no. 3, pp. 184–187, Feb. 1989.

- [55] J. Mahdavi, A. Emadi, and H. A. Toliyat, "Application of state space averaging method to sliding mode control of PWM DC/DC converters," in *Proc. Conf. Rec. IEEE IAS Annu. Meeting*, vol. 2, pp. 820–827, Oct. 1997.
- [56] J. Mahdavi, M. R. Nasiri, and A. Agah, "Application of neural networks and state-space averaging to a DC/DC PWM converter in sliding mode operation," in *Proc. IEEE Conf. IECON*, vol. 1, pp. 172–177, 2000.
- [57] S. C. Tan, Y. M. Lai, M. K. H. Cheung, and C. K. Tse, "An adaptive sliding mode controller for buck converter in continuous conduction mode," in *Proc. IEEE Applied Power Electronics Conf. Expo (APEC)*, pp. 1395–1400, Feb. 2004.
- [58] A. G. Perry, F. Guang, Y. F. Liu, and P. C. Sen, "A new sliding mode like control method for buck converter," in *Proc. IEEE PESC Rec.*, vol. 5, pp. 3688–3693, Jun. 2004.
- [59] L. Iannelli and F. Vasca, "Dithering for sliding mode control of DC/DC converters," in *Proc. IEEE PESC Rec.*, vol. 2, pp. 1616–1620, Jun. 2004.
- [60] S. C. Tan, Y. M. Lai, C. K. Tse, and M. K. H. Cheung, "Adaptive feedforward and feedback control schemes for sliding mode controlled power converters," *IEEE Trans. Power Electron.*, vol. 21, no. 1, pp. 182–192, Jan. 2006.
- [61] Timothy L. Skvarenina, (2001) *The Power Electronics Handbook* (Industrial Electronics series), CRC press.
- [62] S. C. Tan, Y. M. Lai, C. K. Tse, L. Martinez-Salamero, and A. Cid-Pastor, "Design of pulsewidth-modulation based sliding mode controllers for power converters operating in discontinuous conduction mode," *IEEE Industrial Electronics, IECON -2006*, pp. 2769 - 2774.

- [63] S. C. Tan, Y. M. Lai, C. K. Tse, and L. Martinez-Salamero, "Special family of PWM based sliding mode voltage controllers for basic dc-dc converters in discontinuous conduction mode," *Electric Power Applications IET -2007*, vol. 1, no. 1, pp. 64–74.
- [64] Zongqi Hu, Dongsheng Ma, "A pseudo-CCM buck converter with freewheel switching control," *IEEE International Symposium on Circuits and Systems, 2005 (ISCAS 2005)*, Vol. 4, pp. 3083- 3086, May. 2005.
- [65] D. Ma, and W.-H. Ki, "Fast-transient PCCM switching converter with freewheel switching control," *IEEE Trans. Circuits Syst. II*, vol. 54, no. 9, pp. 825–829, Sep. 2007.

BIO-DATA OF THE CANDIDATE

Name: MOUSUMI BISWAL

Father's Name: SUBHRA KESHARI BISWAL

Date of Birth: 27th June 1986

Field of Interest: Power Electronics

Phone: +91 9778411433,

Email: mousumib158@gmail.com

mousumi_biswal@yahoo.com

ACADEMIC QUALIFICATION

- Pursuing M.Tech (Research) in Electrical Engineering, National Institute of Technology, Rourkela.
- B.Tech in Electrical Engineering at Synergy Institute of Engineering and Technology, Dhenkanal.

WORK EXPERIENCE

- One year teaching experience in College of Engineering and Technology, Bhubaneswar.